CSIRO PUBLISHING

Invertebrate Systematics, 2014, **28**, 605–627
http://dx.doi.org/10.1071/IS14003

Phylogenetic relationships within the flatworm genus *Choeradoplana* Graff (Platyhelminthes : Tricladida) inferred from molecular data with the description of two new sympatric species from *Araucaria* moist forests

V. S. Lemos[A,B,C], *G. P. Cauduro*[B], *V. H. Valiati*[B,C] *and A. M. Leal-Zanchet*[A,C,D]

[A]Instituto de Pesquisas de Planárias, Universidade do Vale do Rio dos Sinos – UNISINOS 93022-000, São Leopoldo, RS, Brazil.
[B]Laboratório de Biologia Molecular, Universidade do Vale do Rio dos Sinos – UNISINOS 93022-000, São Leopoldo, RS, Brazil.
[C]Programa de Pós-Graduação em Biologia, Universidade do Vale do Rio dos Sinos – UNISINOS 93022-000, São Leopoldo, RS, Brazil.
[D]Corresponding author. Email: zanchet@unisinos.br

Abstract. The genus *Choeradoplana* encompasses 11 species, nine of which have a restricted distribution and are only known from their type localities. Herein we describe two new species of *Choeradoplana* from Araucaria moist forests, *C. minima*, sp. nov. Lemos & Leal-Zanchet and *C. benyai*, sp. nov. Lemos & Leal-Zanchet, based on morphological and molecular data, and use two molecular markers to investigate their phylogenetic relationships with other species in the genus, including its type species. Both morphological and molecular analyses clearly distinguish *C. minima*, sp. nov., *C. benyai*, sp. nov. and *C. iheringi*. The analyses of the ITS-1, COI and sequence divergence data also indicated that *C. benyai*, sp. nov. is more closely related to the type species of the genus, *C. iheringi*, than to *C. minima*, sp. nov. The three species are sympatric in Araucaria moist forest areas of the São Francisco de Paula National Forest; *C. minima*, sp. nov. and *C. benyai*, sp. nov. seem to be endemic to their type localities. Regarding external morphology, *C. benyai*, sp. nov. and *C. iheringi* could be considered cryptic species, only distinguishable on the basis of the copulatory apparatus. However, immature specimens of *C. benyai*, sp. nov. and *C. iheringi* could only be identified based on molecular data. Our results demonstrate that COI should be used with caution for reconstructing phylogenies, and other slower-evolving nuclear genes are a feasible alternative for resolving some of the phylogenetic relationships.

Additional keywords: Atlantic Forest, Automatic Barcode Gap Discovery, COI, ITS-1, Geoplaninae, land flatworms, taxonomy, triclads.

Received 11 January 2014, accepted 7 September 2014, published online 19 December 2014

Introduction

Land flatworms (Tricladida : Continenticola) are top predators from the soil ecosystem that prey upon other invertebrates (Du Bois-Reymond Marcus 1951; Froehlich 1955*a*; Ogren 1995; Jones and Cumming 1998; Carbayo and Leal-Zanchet 2003; Prasniski and Leal-Zanchet 2009). These flatworms have restricted locomotion capacity over long distances, so there are many endemic species (Sluys 1995). Their behaviour is cryptic and depends on the moisture of their microhabitat because they do not have water-saving adaptations (Kawaguti 1932; Froehlich 1955*a*; Winsor *et al*. 1998). These characteristics force them to remain hidden during the day in humid refuges, such as the leaf litter and under stones or fallen logs and branches (Antunes *et al*. 2012). Land triclads select relatively undisturbed areas, such as native forests and plantations of a native species in southern Brazil, rather than plantations of exotic species (Carbayo *et al*. 2002; Fonseca *et al*. 2009; Oliveira *et al*. 2014). However, they do not show signs of microhabitat selection in pristine Araucaria moist forests (Antunes *et al*. 2012).

Areas of Araucaria moist forest (Mixed Ombrophilous Forest) located in the Araucaria Plateau, in southern Brazil, belong to the Atlantic Forest biome and harbour a high diversity of land flatworms (Leal-Zanchet and Carbayo 2000; Carbayo *et al*. 2002; Leal-Zanchet and Baptista 2009; Leal-Zanchet *et al*. 2011). The São Francisco de Paula National Forest is one of these areas and was originally covered by Araucaria moist forest and native grasslands. This area was indicated as the type locality for various species of different Geoplaninae genera (Leal-Zanchet and Carbayo 2001; Carbayo

and Leal-Zanchet 2001, 2003; Baptista and Leal-Zanchet 2005; Lemos and Leal-Zanchet 2008; Amaral *et al*. 2012; Leal-Zanchet *et al*. 2012), where they seem to be randomly distributed (Antunes *et al*. 2012). One of these genera is *Choeradoplana* Graff, 1896 (Leal-Zanchet and Carbayo 2000; Leal Zanchet *et al*. 2011).

Choeradoplana was proposed by Graff (1896) and reviewed by Froehlich (1955*b*). More recently, Carbayo and Leal-Zanchet (2003) and Carbayo and Froehlich (2012) proposed an emendation of its diagnosis. This genus is relatively well defined, its specimens presenting a cephalic region with a glandulo-muscular organ and longitudinal cutaneous musculature with a portion sunk into the mesenchyme.

This genus encompasses 11 species, nine of which have a restricted distribution and are only known from their type localities (Ogren and Kawakatsu 1990; Carbayo and Froehlich 2012; Negrete and Brusa 2012). Two other species, *C. iheringi* Graff, 1899 and *C. langi* (Graff, 1894), have a relatively ample distribution and have been recorded in Argentina and southern Brazil (Graff 1899; Ogren and Kawakatsu 1990; Leal-Zanchet and Souza 2003).

Currently, land flatworms belong to the family Geoplanidae, which is subdivided into four subfamilies, viz. Bipaliinae, Microplaninae, Rhynchodeminae and Geoplaninae (Sluys *et al*. 2009), as proposed by Carranza *et al*. (1998). The latter has a Neotropical distribution and comprises ~260 species in 23 genera (Sluys *et al*. 2009; Carbayo *et al*. 2013). In a recent attempt to test the monophyly of Geoplaninae, based on molecular data, species of 20 genera were analysed by Carbayo *et al*. (2013). According to their results, species of the genera *Choeradoplana* and *Cephaloflexa* form a monophyletic group.

Although taxonomic descriptions of land flatworms have largely been based on morphological characters, here we describe two new species of *Choeradoplana* from Araucaria moist forests based on morphological and molecular data. In addition we use these two molecular markers to investigate their phylogenetic relationships with the type species of the genus and other closely related species.

Materials and methods

Specimens of *C. minima*, sp. nov. Lemos & Leal-Zanchet and *C. benyai*, sp. nov. Lemos & Leal-Zanchet were collected from São Francisco de Paula (São Francisco de Paula National Forest) (29°23′–29°27′S; 50°23′–50°25W), located in the state of Rio Grande do Sul, Brazil. Sampling took place mainly in areas of Mixed Ombrophilous Forest and plantations of the native *Araucaria angustifolia* (Bertol.) O. Kuntze. One exemplar of *C. minima*, sp. nov. was collected in a *Pinus* spp. plantation. Specimens were collected during the day by direct sampling in leaf litter and under fallen logs and stones. The specimens collected, locality data, and identification and GenBank accession numbers are listed in Table S1.

DNA isolation, PCR amplification and DNA sequencing

Genomic DNA was isolated from 15 specimens of *Choeradoplana* and 3 specimens of other two Geoplaninae genera, *Supramontana* and *Matuxia*, preserved in ~100% ethanol (Table S1) using the Wizard® Genomic DNA Purification Kit (Promega, Madison, WI, USA) according to the manufacturer's instructions. We amplified a 950 bp fragment of the cytochrome *c* oxidase subunit I (COI) gene with the primers BarT (5′-ATG ACD GCS CAT GGT TTA ATA ATG AT-3′) (Álvarez-Presas *et al*. 2011) and COIR (5′-CCW GTY ARM CCH CCW AYA GTA AA-3′) (Lázaro *et al*. 2009). For the nuclear fragment ITS-1, we amplified ~500 bp using the primers ITS9F (5′-GTA GGT GAA CCT GCG GAA GG-3′) and ITSR (5-TGC GTT CAA ATT GTC AAT GAT C-3′) from Baguñà *et al*. (1999). The same primers were used for sequencing. The PCR amplification for both markers (COI and ITS-1) was carried out in a total volume of 25 µL or 50 µL, including 20–50 ng of genomic DNA, 0.2 µM of each primer, 200 µM dNTPs, 1× buffer, 1.5 mM $MgCl_2$, 1 unit of Taq DNA polymerase (Invitrogen, USA) and ultrapure H_2O to make up the remainder of the reaction volume. The conditions for amplify the COI mitochondrial gene were 95°C for 3 min (denaturation), 38 cycles of 50 s at 94°C (denaturation), 55 s at 43°C (annealing) and 68 s at 68°C (extension). The reaction was then incubated at 60°C for 5 min for the final extension step. The amplification conditions for ITS-1 were 94°C for 4 min (denaturation), 36 cycles of 60 s at 94°C (denaturation), 40 s at 45°C (annealing) and 1 min at 72°C (extension). The reaction was then incubated at 72°C for 6 min for the final extension step.

Sequence and phylogenetic analysis

Quality of sequences was evaluated by verifying the chromatogram in ChromasPro 1.5 software (http://www.technelysium.com.au). Sequences were also checked using the BLASTn on-line tool for comparison with sequences deposited in the GenBank database (NCBI). Sense and antisense sequences for each specimen were aligned by MAFFT (Katoh and Toh 2008) using the E-INS-i algorithm manually inspected and, when necessary, corrected using BioEdit 5.0.9 (Hall 1999) to obtain the consensus sequence. The amino acid translation was examined to ensure that no gaps or stop codons were present in the alignment. Due to sequence length variation in ITS-1, Gblocks (Talavera and Castresana 2007) was used to remove fragments of ambiguous alignment, to be subsequently used in the phylogenetic analyses.

Phylogenetic analyses were conducted using PHYML 2.4.4 (Guindon and Gascuel 2003) for maximum likelihood (ML) and MrBayes 3.1.2 (Ronquist and Huelsenbeck 2003) for Bayesian inference of phylogeny (BI). For ML, the most likely topology was calculated based on Shimodaira-Hasegawa test (Sh-like) implemented in PhyML. For BI, the Markov chain Monte Carlo search was run with 10 000 000 generations (repeated two times), sampled in every 1000 generations, discarding the first 25% trees as 'burn-in,' after which the chain reached stationarity, which ensured that the average split frequencies between the runs was less than 1%. These analyses were performed for each gene and on a combined matrix of genes. MODELTEST (Posada and Crandall 1998) was used in order to select the best-fit model of sequence evolution under the

Akaike Information Criterion (AIC) (Akaike 1974). For the COI gene, the best-fit model was GTR + I + G (Rodríguez *et al*. 1990). For the ITS-1 gene the best-fit model was HKY + I + G (Hasegawa *et al*. 1985).

Clade support for the maximum likelihood analyses was based on 1000 bootstrap replicates (Felsenstein 1985) whereas for the Bayesian inferences the posterior probability (PP) of each clade on the 50% majority rule consensus tree was measured. Additionally, for the COI gene, Bayesian inference was conducted clustering together the first and second positions of each codon in one single partition. We used MODELTEST (Posada and Crandall 1998) to select the most appropriate evolutionary model of sequence evolution (GTR + G) under the AIC criterion.

The Bayesian and ML analyses of the concatenated mitochondrial and nuclear datasets were partitioned by genes, assuming as the best fit-model the same model provided by AIC for individual gene analyses and branch lengths inferred jointly for each partition. In addition, pairwise nucleotide distances between all sequences were calculated according to Kimura's 2-parameter model and 1000 bootstrap replications (Kimura 1980) using MEGA version 5.1. Saturation of nucleotide substitution in the COI gene dataset was checked using the number of transitions and transversions versus divergence, performed on DAMBE 5.0.25 (Xia and Xie 2001) with Kimura's two-parameter distance (Kimura 1980). We used three different datasets considering: (1) the three codon positions; (2) the first and second positions; and (3) only the third codon position.

The Automatic Barcode Gap (ABGD) tool (Puillandre *et al*. 2012) was used for species delimitation analysis. ABGD automatically detects breaks in the distribution of genetic pairwise distances, referred to as the 'barcode gap' and uses it to partition of the data. COI and ITS-1 distance matrices produced by MEGA were uploaded to http://wwwabi.snv.jussieu.fr/public/abgd/abgdweb.html and ABGD was run with default settings, namely Pmin = 0.001, Pmax = 0.1, Steps = 10, X (relative gap width) = 15, Nb bins = 20, and with K2P distances. The program requires two user-specified values: P (prior limit to intraspecific diversity) and X (proxy for minimum gap width). Prior maximum intraspecific divergences included thresholds between 0.001 to 0.6.

Techniques for morphological analyses of the type material

Methods described by Froehlich and Leal-Zanchet (2003) were used for histological processing of material and analysis of external and internal characters. The material was sectioned at 5–7 µm.

The ratio of the height of the cutaneous musculature to the height of the body (mc:h index in Froehlich 1955*b*) was determined in the median region of a transverse section of the pre-pharyngeal region. Mesenchymal muscle fibres were counted in transverse sections of the same region. Colour descriptors, based on the uptake of dyes of particular colours, were used for classifying secretions with trichrome methods: erythrophil, xanthophil and cyanophil. The term cyanophil is also applied to secretions that have an affinity for the green dye of Goldner's Masson.

Type material was deposited in the following reference collections: Museu de Zoologia da Universidade do Vale do Rio dos Sinos, São Leopoldo, Rio Grande do Sul, Brazil (MZU), and the Helminthological Collection of Museu de Zoologia da Universidade de São Paulo, São Paulo, São Paulo State, Brazil (MZUSP).

Results

Phylogenetic relationships within Choeradoplana

The monophyly of the genus *Choeradoplana* and its sister group *Cephaloflexa* was recovered when we used the ITS-1 gene (Fig. 1) and when the genes ITS-1 and COI were concatenated (Online Resource 1). On the other hand, the phylogenetic trees generated from ML and Bayesian inferences (Fig. 2), using only the COI gene, do not recover the monophyly of these genera. Bayesian and ML analyses of the concatenation of mitochondrial and nuclear datasets provide highly congruent and globally well resolved topologies (Online Resource 1) that are very similar to the ones based on ITS-1 alone (Fig. 1).

The saturation test for the COI gene revealed a clear sign of rapid saturation of transitional substitutions in the third codon positions with low genetic divergence (< 3%). On the other hand, the transitions curve appears to become partially saturated above the 6% divergence when considering only the 1st and 2nd positions and < 3% regarding only the 3rd position. Third codon positions showed saturation, since their Iss values do not differ statistically from their Iss.c (Iss = 0.518; Iss.c = 0.634; $P = 0.088$). However, when only the first two codon positions were used, we perceive no further significant saturation (Iss = 0.035; Iss.c = 0.694; $P < 0.001$). The nucleotide substitution rates (Table S2) for COI gene showed that intrageneric differences are smaller than the saturation levels when we consider only the first two codon positions. The genus *Cephaloflexa* is an exception since its nucleotide substitution rates are 8.7%. Therefore, the results suggest that the COI sequences of this genus have undergone substitution saturation throughout speciation, which led to the loss of the original phylogenetic signal, producing a polytomy (Fig. 2 and Online Resource 2). Likewise, all comparisons showed interspecific differences above the saturation level (Table S2), which demonstrates that COI should be used with caution for reconstructing phylogenies and suggests the use of slower-evolving nuclear genes for resolving some of the phylogenetic relationships. Despite the small number of available taxa, the use of an ITS-1 region demonstrated that interspecific differences (Table S3) supported relationships recovered in Bayesian analysis and maximum likelihood, which were not completely observed when using only the COI gene (Fig. 2).

The ITS-1 differences among the new species herein described, *C. minima*, sp. nov. and *C. benyai*, sp. nov., and the type species of *Choeradoplana*, *C. iheringi*, clearly indicate the molecular distinction of these three units. Likewise, our measures of intraspecific and interspecific variation of the

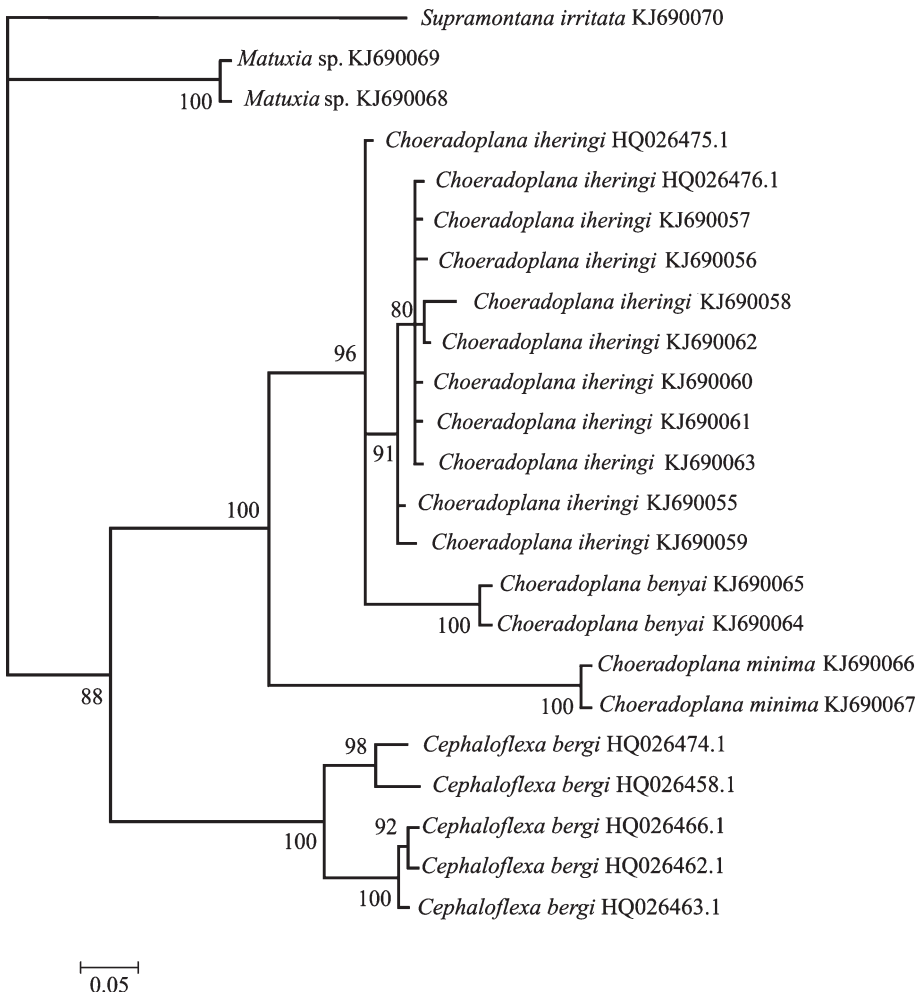

Fig. 1. Bayesian tree obtained from all sequence data (ITS-1) of *Choeradoplana* species and other related taxa. Numbers on branches are Bayesian posterior probabilities (only values above 70% are shown). GenBank accession numbers are shown after the name of the taxa.

COI gene and the method to split a sequence dataset into candidate species (Automatic Barcode Gap Discovery - ABGD), by using the ITS-1 and COI (Online Resources 3 and 4, respectively), enable the separation of them as evolutionarily independent species belonging to the genus *Choeradoplana.* ABGD applied to the ITS-1 gene indicated that *C. minima* and *C. benyai*, as well as *C. iheringi*, constitute monophyletic groups, based on an intraspecific threshold of 6% genetic divergence and including recursive evaluation of group splitting (Online Resource 3). In the case of the COI gene, with a larger available dataset, ABGD indicated the distinction of seven species of *Choeradoplana* (*C. iheringi*, *C. albonigra*, *C. bocaina*, *C. banga*, *C. minima*, sp. nov., *C*, *benyai*, sp. nov. and *C. gladismariae*), with intraspecific divergences of 4% (Online Resource 4). Both analyses as well as sequence divergence data (Tables S2 and S3) indicated that *C. benyai*, sp. nov. is more closely related to the type species of the genus, *C. iheringi*, than to *C. minima*, sp. nov.

Description of the species

Phylum **PLATYHELMINTHES** Minot, 1876

Order **TRICLADIDA** Lang, 1884

Family **GEOPLANIDAE** Stimpson, 1857

Subfamily **GEOPLANINAE** Stimpson, 1857

Genus *Choearadoplana* Graff, 1896

Choeradoplana minima , sp. nov. Lemos & Leal-Zanchet

Choeradoplana sp. 2: Leal-Zanchet & Carbayo, 2000: 23.
Choeradoplana sp. 1: Leal-Zanchet & Baptista, 2009: 202.
Choeradoplana sp. 2: Leal-Zanchet, Baptista, Campos & Raffo, 2011: 32.
Choeradoplana sp.: Antunes, Leal-Zanchet & Fonseca, 2012: 27.

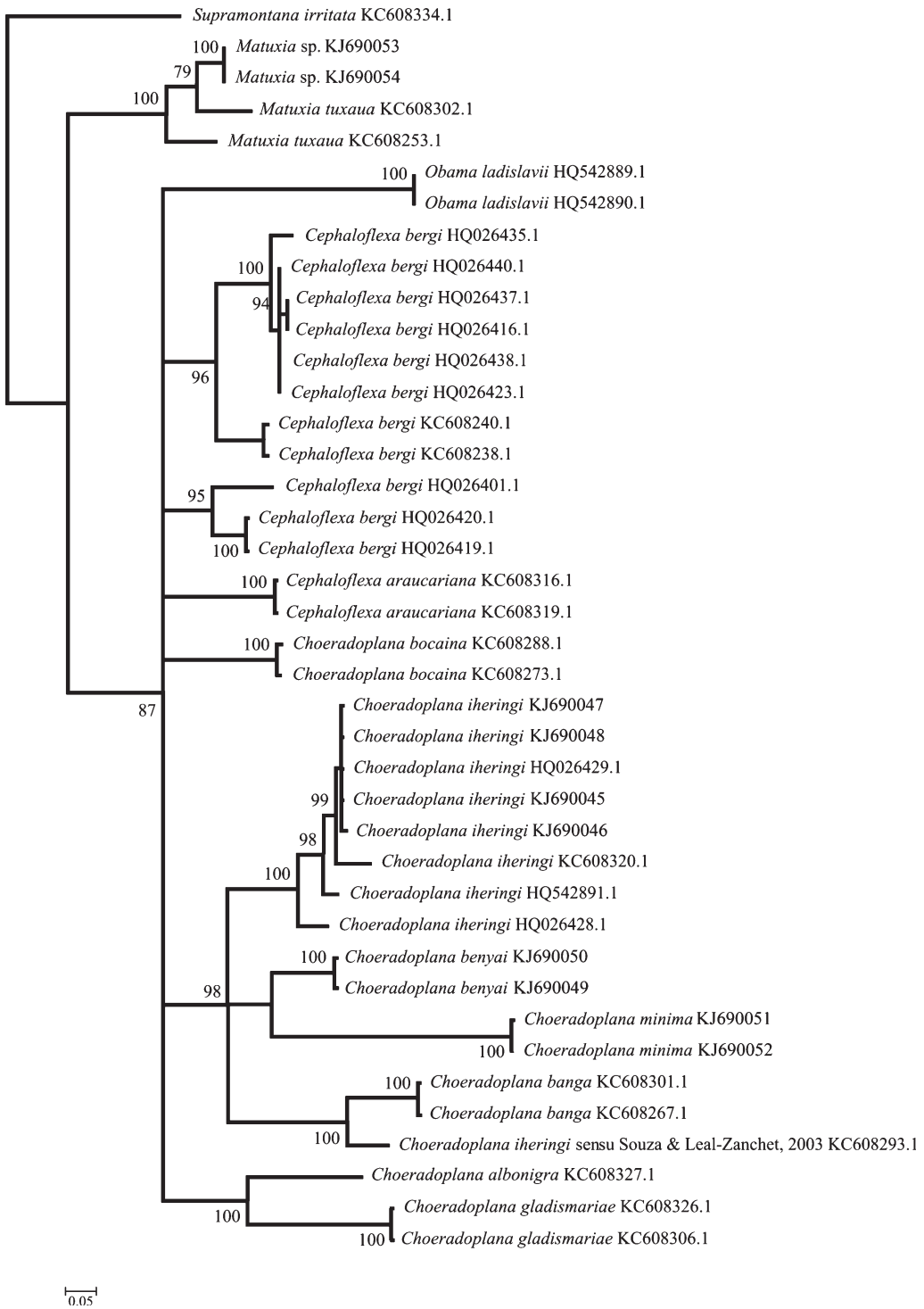

Fig. 2. Maximum likelihood phylogenetic tree of *Choeradoplana* species and other related taxa. Topology based on the first 822 bp of the COI gene. Numbers on branches indicate the percentage of 1000 bootstrap replicates that supported the branch (only values above 70% are shown). GenBank accession numbers are shown after the name of the taxa.

Type material

Holotype. MZUSP PL. 1234: I. A. Fick, *leg*. 14. VII. 2000: São Francisco de Paula, RS, Brazil – anterior tip in two fragments: transverse sections on 16 slides and sagittal sections on 3 slides; anterior region at the level of ovaries: horizontal sections on 8 slides; pre-pharyngeal region: transverse sections on 4 slides;

pharynx: sagittal sections on 4 slides; copulatory apparatus: sagittal sections on 7 slides.

Paratypes. MZU PL.00138: I. A. Fick, *leg*. 10. XII. 1998: São Francisco de Paula, RS, Brazil – anterior tip: transverse sections on 5 slides; pre-pharyngeal region in two fragments: transverse sections on 9 slides; pharynx and copulatory apparatus in two fragments: sagittal sections on 25 slides; MZU PL.00139: I. A. Fick, *leg*. 21. XII. 1998: São Francisco de Paula, RS, Brazil – pre-pharyngeal region: transverse sections on 6 slides; pharynx and copulatory apparatus: sagittal sections on 10 slides; MZU PL.00140: M. Cardoso, *leg*. 14. I. 1999: São Francisco de Paula, RS, Brazil – pharynx and copulatory apparatus: sagittal sections on 7 slides; MZU PL.00141: F. Carbayo, *leg*. 23.02.1999: São Francisco de Paula, RS, Brazil – anterior tip: sagittal sections on 9 slides; pre-pharyngeal region: transverse sections on 5 slides; pharynx: sagittal sections on 4 slides; copulatory apparatus: sagittal sections on 11 slides; MZU PL.00143: P. K. Boll, *leg*. 25. II. 2010: São Francisco de Paula, RS, Brazil – anterior tip: transverse sections on 144 slides; pre-pharyngeal region: transverse sections on 93 slides; pharynx and copulatory apparatus: sagittal sections on 166 slides; posterior fragment preserved in ethanol 100% for molecular analyses; MZU PL.00144: J. Braccini, *leg*. 09. VI. 2011: São Francisco de Paula, RS, Brazil – anterior tip: transverse sections on 4 slides; pre-pharyngeal region: transverse sections on 8 slides; pharynx and copulatory apparatus: sagittal sections on 10 slides; posterior fragment preserved in ethanol 100% for molecular analyses; MZU PL.00145: G. G. Iturralde, *leg*.09. VI. 2011: São Francisco de Paula, RS, Brazil – pre-pharyngeal region: transverse sections on 6 slides; pharynx and copulatory apparatus: sagittal sections on 21 slides; posterior fragment preserved in ethanol 100% for molecular analyses.

Type locality:

São Francisco de Paula, state of Rio Grande do Sul (RS), Brazil.

Diagnosis

Dorsal surface with two wide paramedian stripes formed by dark-brown pigmentation; mc:h, 10%–12%; anteriormost testes posterior to ovaries, posteriormost testes near root of

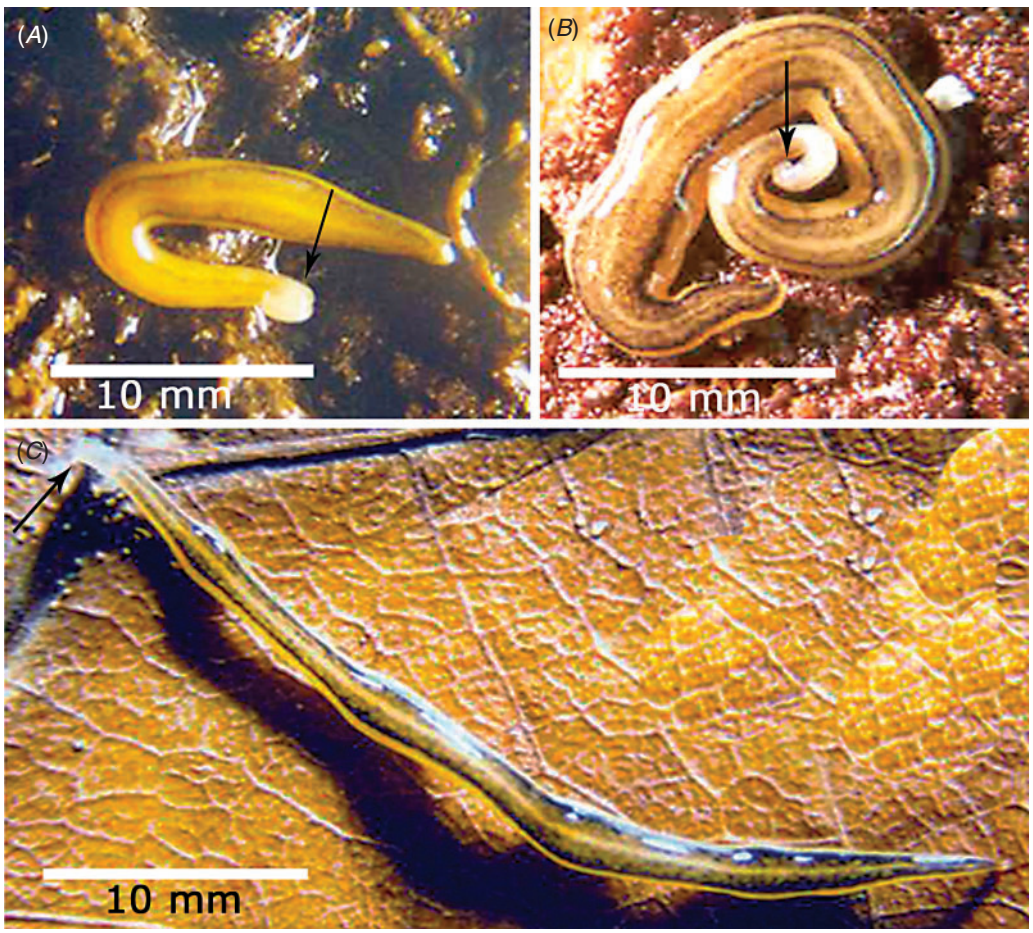

Fig. 3. *Choeradoplana minima*, sp. nov. Lemos & Leal-Zanchet. Photograph of live specimens in dorsal view: (*A*) paratype MZU PL. 00140; (*B*) paratype MZU PL.00139; (*C*) paratype MZU PL. 00138. Arrows indicate the anterior tip.

pharynx; ejaculatory cavity short, with folded wall and sinuous lumen; inverted penis with strong bulbar musculature, well developed muscularis and two main regions; male atrium short occupied by the tip of the inverted penis; ovovitelline ducts emerging laterally from median third of ovaries, and ascending behind the gonopore; male and female atria with independent musculatures and with wide communication at the sagittal plane.

Description

External morphology

Body elongate with parallel margins (Figs 3–4), subcylindrical in cross-section; anterior end obtuse, posterior end pointed. Cephalic region (less than 1 mm long and 0.5 mm wide) with two glandular cushions and a median slit in the ventral surface (Fig. 4*C*). When crawling, maximal length reaches 34 mm (Table 1). Mouth distance from anterior tip, 58%, gonopore distance from anterior tip, 71% relatively to body length in the holotype (Table 1).

Alive, dorsal surface with two wide paramedian stripes formed by dark-brown pigmentation, darker on their external border (Figs 3, 4*A*). Ground colour pale yellow, visible on the median region and margins of the body. Ventral surface yellowish; whitish on cephalic region. After fixation, the cephalic region is pale yellow dorsally and ventrally, excepting for the ventral glandular cushions that are brownish. The paramedian stripes begin at the end of the cephalic region. They begin narrow, becoming posteriorly broader, accompanying the enlargement of the body towards the median third of the body. The paramedian stripes cover 0.25 mm of the dorsal surface on each side of the body, corresponding to 40% of body width in the median third of the body in paratype MZU PL.00140 (Figs 3*A*, 4). Near posterior end stripes gradually become narrower and converge (Fig. 4*A*). Ventral surface pale yellow.

Sensorial border visible between the 0.3 mm and 1.5 mm of the body. Eyes are uniserial and marginal in the whole body length excepting the first 0.3 mm, where they are absent (Fig. 4). The anteriormost eyes are monolobated, occurring intercalated with trilobated eyes after the first millimetre of the body. Towards posterior end, eyes become sparser, occurring until next to the posterior tip (Fig. 4*A*). No unpigmented areas (clear halos) surrounding eyes.

Internal morphology

Sensory organs, cutaneous and mesenchymal musculatures and epidermis

Sensory pits, as simple invaginations (Fig. 5*C*), ~20 µm to 25 µm deep, absent on anterior tip, occurring in a single row between 0.6 mm and 4 mm from anterior tip. They occur initially at intervals of 30 µm. Eyes ~40 µm in diameter.

Cutaneous musculature with the usual three layers (circular, oblique and longitudinal layers), but with the ventral longitudinal layer partially insunk in the mesenchyme (Table 2, Fig. 5*A*, B). In addition, a few fibres of the dorsal longitudinal layer are also insunk in the mesenchyme. The longitudinal layer is approximately between three and six times higher than the other two in the pre-pharyngeal region (Table 2). Cutaneous musculature slightly higher paramedially than medially. Ventral musculature higher than the dorsal

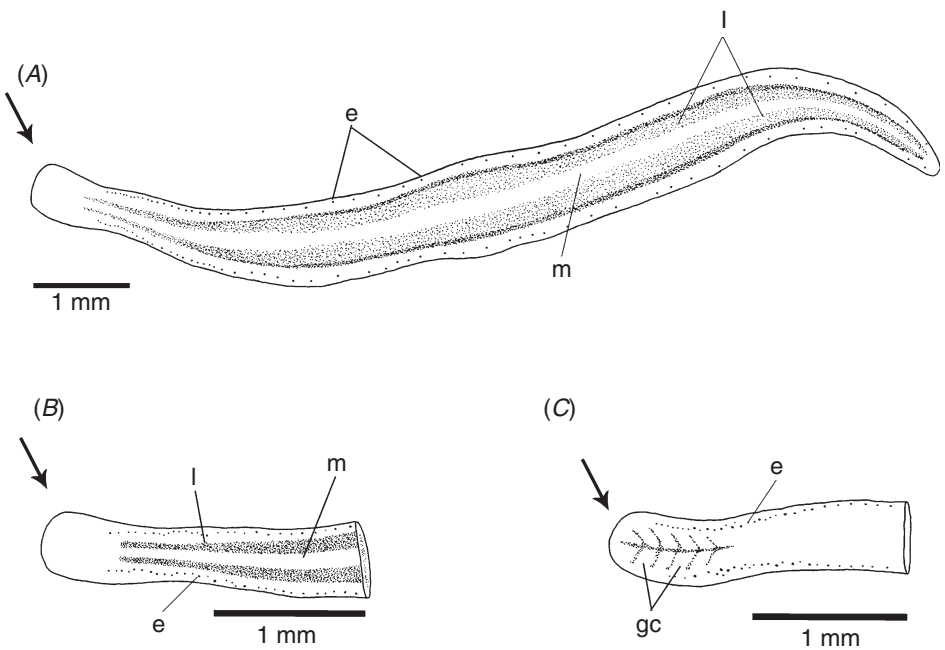

Fig. 4. *Choeradoplana minima*, sp. nov. Lemos & Leal-Zanchet (paratype MZU PL. 00140): (*A*) colour pattern in dorsal view; (*B*) detail of eyes pattern of the anterior body third in dorsal view; (*C*) detail of the glandular cushions in the cephalic region in ventral view. Arrows indicate the anterior tip. e, Eyes; gc, glandular cushions; l, lateral stripes; m, median stripe.

Table 1. Measurements, in millimetre, of specimens of *Choeradoplana minima*, sp. nov. Lemos & Leal-Zanchet

–: not measured; *: After fixation; **: specimens with damaged anterior tip (lost or regenerating); DG: distance of gonopore from anterior end; DM: distance of mouth from anterior end; DMG: distance between mouth and gonopore; DPVP: distance between prostatic vesicle and pharyngeal pouch. The numbers given in parentheses represent the position relative to body length

	Holotype MZUSP PL. 1234	Paratype MZU PL. 00138	Paratype MZU PL. 00139	Paratype MZU PL. 00140	Paratype MZU PL. 00141	Paratype MZU PL. 00143	Paratype MZU PL.00144	Paratype MZU PL. 00145
Maximum length in extension	21	25	26	15	34	–	21	18
Maximum width in extension	1.5	1.25	1	1	1.5	–	1	2
Length at rest	12.2	13	10	8	13	12	16	9
Width at rest	2	1.5	3	1	2.5	1	2	4
Length*	19	16	21	9	20	10.5	18	–
Width*	1.5	1	1.5	0.8	1.8	1	1.5	0.7
DM*	11 (58)	7 (44)	12 (57)	5 (55)	9 (45)	6 (57)	12.5 (69)	–
DG*	13.5 (71)	5.5 (34)	15 (71)	6 (67)	14.5 (72)	7 (67)	13.5 (75)	–
DMG*	2.5	2.5	3	1	2.5	1	1	–
DPVP*	0.8	0.6	0.6	–	0.9	–	0.6	–
Creeping sole %	67	60	87	–	66	80	33	92
Ovaries	6.6 (35)	–	–	–	–	–	–	–
Anteriormost testes	6.8 (36)	–	–	–	3.9 (19)	–	–	–
Posteriormost testes	10.4 (55)	9.9 (62)	–	5 (55)	–	4.8 (46)	6.8 (38)	–
Prostatic vesicle	0.3	0.3	0.3	–	0.2	–	0.2	–
Inverted penis	0.9	1.2	1.0	–	0.8	–	–	–
Male atrium	0.2	0.2	0.2	–	0.1	–	–	–
Female atrium	0.7	0.6	0.8	–	0.8	–	0.6	–
Vagina	0.2	0.2	0.1	–	0.2	–	0.11	–
Common ovovitelline duct	0.1	0.2	0.2	–	0.2	–	0.3	–

in the pre-pharyngeal region. Mc:h 12% in the holotype (Table 2). The dorsal cutaneous musculature is thinner next to the anterior tip, whereas the ventral cutaneous musculature is higher and with the longitudinal layer totally insunk in the mesenchyme, located below cell bodies of glands opening through ventral epidermis, forming the retractor muscle (Fig. 5*C*, *D*).

Mesenchymal musculature weakly developed with variously oriented fibres, mainly forming three layers: oblique dorsal (~2 fibres thick), supra-intestinal transverse (~4–6 fibres thick) and sub-intestinal transverse (~4–6 fibres thick). In addition, dorsoventral fibres are present. Longitudinal fibres are indiscernible. Fibres of the oblique dorsal and supra-intestinal layers form a dorsal muscle net ('Muskelgeflecht') in the cephalic region. The sub-intestinal transverse layer is thicker in the cephalic region than in the pre-pharyngeal region and interwoven with the fibres of the insunk ventral cutaneous musculature in the retractor muscle (Fig. 5*C*, *D*).

Width of creeping sole, 67% of body width in the holotype (Table 1). A slit occurs between the two glandular cushions in the cephalic region, representing the beginning of the creeping sole from 0.3 mm to 1.3 mm from anterior tip. Four types of secretory cells open through dorsal epidermis and body margins: (1) numerous rhabditogen cells with xanthophil secretion (rhammites); (2) sparse cells with fine granular, erythrophil secretion; (3) cells with mixed secretion (an erythrophil central core and a cyanophil peripheral part); (4) few cells with amorphous, cyanophil secretion. Creeping sole receives abundant amorphous cyanophil secretion and scarce fine granular xanthophil secretion. Few rhabditogen cells with small, xanthophil rhabdites and cells with mixed secretion also discharge through the creeping sole. There is no glandular margin (Fig. 5*A*). Three gland types (rhabditogen cells, erythrophil cells and cyanophil cells) also open through the epidermis of the anterior tip, but rhabditogen cells with rhammites open on ventral surface and body margins and the rhabditogen cells with smaller rhabdites on dorsal surface. Cell bodies of the glands opening on ventral surface are located between the retractor muscle and ventral epidermis forming the musculo-glandular organ next to the anterior tip (Fig. 5*C*, *D*).

Pharynx

Pharynx bell-form with almost unfolded external wall. Mouth in the end of median third of pharyngeal pouch, slightly posterior to the dorsal insertion. Oesophagus absent (Fig. 5*E*). Pharynx and pharyngeal lumen lined by cuboidal to columnar ciliated epithelium showing some insunk nuclei; the insunk nuclei of the epithelium of the pharyngeal lumen are located immediately subepithelially or among fibres of inner pharyngeal musculature. Four types of pharyngeal glands, three of which with coarse granular secretion (xanthophil, erythrophil and mixed secretion) and one with amorphous cyanophil secretion. The mixed secretion is composed by an erythrophil core and a cyanophil peripheral part. Xanthophil and erythrophil cells are the most numerous. Cell bodies of pharyngeal glands located in the mesenchyme, mainly anterior and posteriorly to pharynx. Outer musculature of pharynx (~25 µm thick) constituted of thin longitudinal subepithelial layer, followed by a thicker circular one, mixed internally with few longitudinal fibres. Towards pharyngeal tip, circular layer

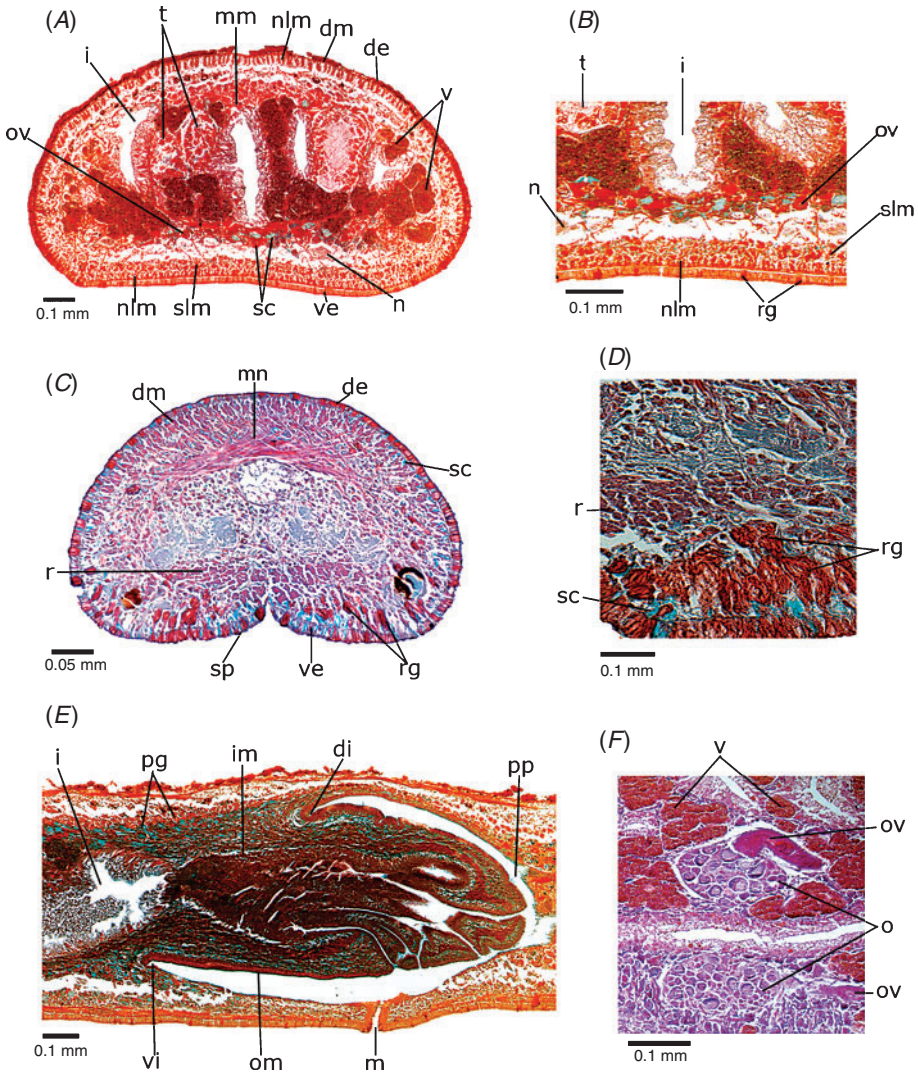

Fig. 5. *Choeradoplana minima*, sp. nov. Lemos & Leal-Zanchet (holotype) in (*A–D*) transverse, (*E*) sagittal sections or (*F*) horizontal sections: (*A*) pre-pharyngeal region; (*B*) detail of the ventral surface of the pre-pharyngeal region; (*C*) anterior region of the body; (*D*) detail of ventral surface of the anterior region of the body; (*E*) pharynx; (*F*) ovaries. Anterior tip to the left (*E–F*). de, Dorsal epidermis; di, dorsal insertion; dm, dorsal cutaneous musculature; i, intestine; im, inner pharyngeal musculature; m, mouth; mm, mesenchymal muscles; mn, muscle net; n, nerve plate; nlm, normal longitudinal cutaneous muscles; om, outher musculature of pharynx; o, ovary; ov, ovovitelline duct; pg, pharyngeal glands; pp, pharyngeal pouch; r, retractor muscle; rg, rhabditogen cells; sc, secretory cells; sp, sensory pits; slm, sunken longitudinal cutaneous muscles; t, testes; v, vitellaria; ve, ventral epidermis; vi, ventral insertion.

becomes as thin as longitudinal one. Inner pharyngeal musculature (~40 µm thick) composed of thick circular subepithelial layer mixed with some longitudinal fibres. Inner musculature gradually becomes thinner outwards and inwards.

Reproductive apparatus

Testes in two irregular rows on each side of the body, beneath the dorsal transverse mesenchymal muscles, embedded between intestinal branches (Fig. 5*A*). They extend just behind to the ovaries to just anterior of the pharynx (Table 1). Pre-pharyngeally, sperm ducts dorsal to ovovitelline ducts, medially displaced. They form spermiducal vesicles slightly posterior to pharynx. Spermiducal vesicles enter common muscle coat, ascend slightly and recurve to open into the proximal wall of prostatic vesicle (Figs 6, 7). Before its opening, each spermiducal vesicle expands in diameter, forming a round distal portion. Intrabulbar prostatic vesicle globose, with folded wall and narrow lumen (Table 1, Figs 6, 7). The prostatic vesicle opens through a short ejaculatory cavity into the lower part of the cavity of the inverted penis (Figs 6, 7, 8*A*). Ejaculatory cavity with folded wall and sinuous lumen. Inverted penis with two main regions, the proximal half with a tubular form and an ample cavity without folds; the distal half

Table 2. Cutaneous musculature and body height, in micrometre, in the median region of a transverse section of the pre-pharyngeal region, and ratio of the height of cutaneous musculature to the height of the body (mc:h index) of specimens of *Choeradoplana minima*, sp. nov. Lemos & Leal-Zanchet

	Holotype MZUSP PL. 1234	Paratype MZU PL. 00138	Paratype MZU PL. 00139	Paratype MZU PL. 00141	Paratype MZU PL. 00144	Paratype MZU PL. 00145
Dorsal circular	2	2.4	1.6	2	1.6	1.6
Dorsal oblique	5	3.2	4	5	2.4	2.4
Dorsal longitudinal	25	24	23.2	24	18.4	26.4
Dorsal total	32	29.6	28.8	31	22.4	30.4
Ventral circular	4	2.4	1.6	2	1.6	1.6
Ventral oblique	2	1.6	2.4	4	4	3.2
Ventral longitudinal	19	16	14.4	17	9.6	18.4
Ventral insunk	16	18.4	12	14	5.6	15.2
Ventral total	41	38.4	30.4	37	20.8	38.4
Body height	625	720	600	625	710	340
Mc:h (%)	12	9	10	11	6	13

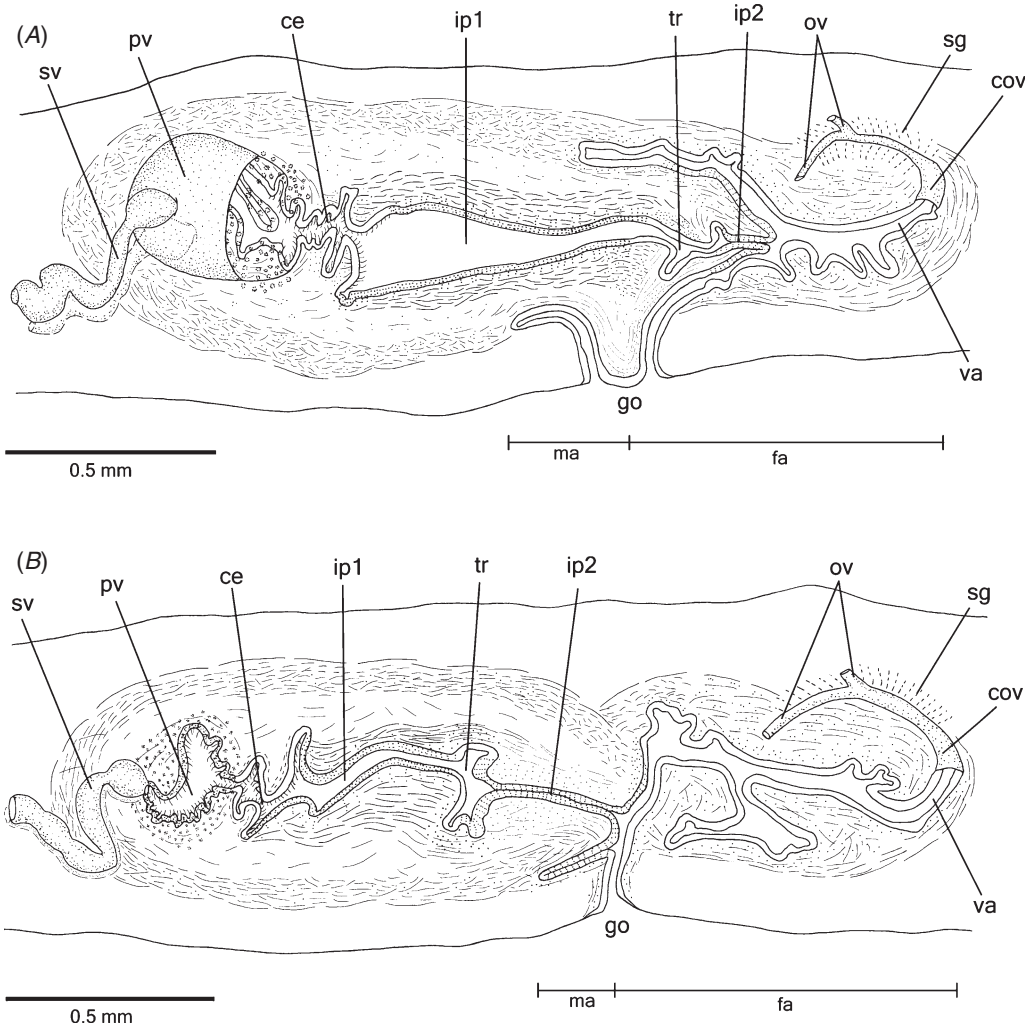

Fig. 6. *Choeradoplana minima*, sp. nov. Lemos & Leal-Zanchet: sagittal composite reconstruction of the copulatory apparatus of the (*A*) holotype and (*B*) paratype MZU PL.00141. Anterior tip to the left. cov, Common glandular ovovitelline duct; ec, ejaculatory cavity; fa, female atrium; go, gonopore; ip1, proximal half of the inverted penis; ip2, distal half of the inverted penis; ov, ovovitelline ducts; pv, prostatic vesicle; ma, male atrium; sg, shell glands; sv, spermiducal vesicle; tr, transition region; va, vagina.

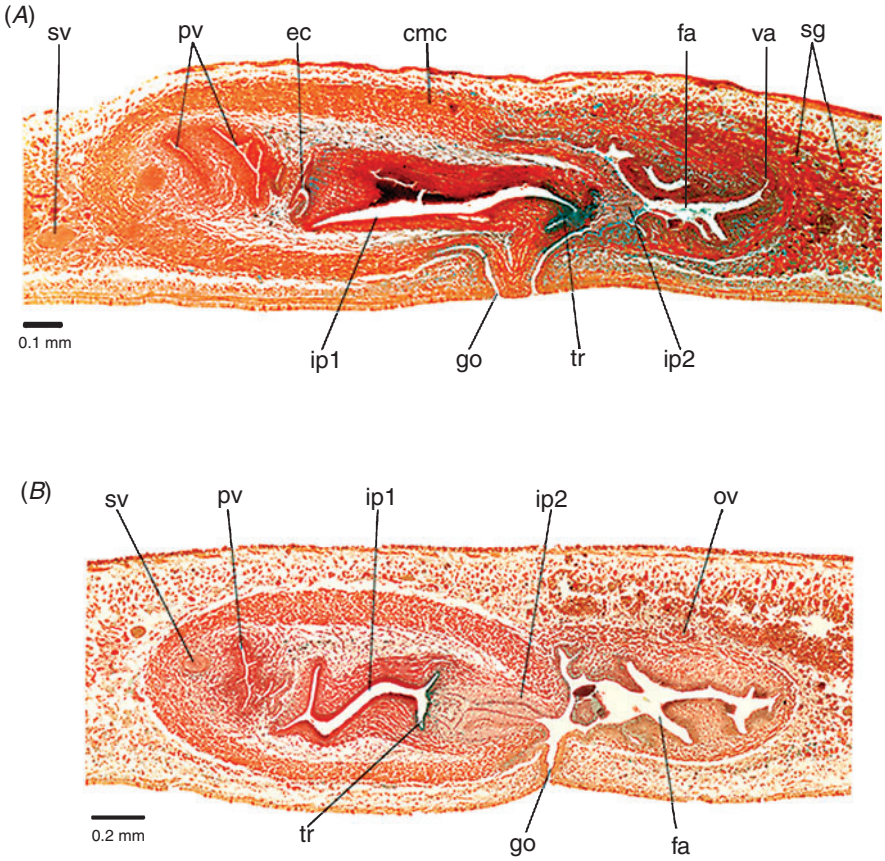

Fig. 7. *Choeradoplana minima*, sp. nov. Lemos & Leal-Zanchet: copulatory apparatus of the (*A*) holotype and (*B*) paratype MZU PL.00141 in sagittal sections. Anterior tip to the left. cmc, Common muscle coat; ec, ejaculatory cavity; fa, female atrium; go, gonopore; ip1, proximal half of the inverted penis; ip2, distal half of the inverted penis; ov, ovovitelline ducts; pv, prostatic vesicle; sg, shell glands; sv, spermiducal vesicle; tr, transition region; va, vagina.

forms a short circular fold with narrow lumen. Male atrium short, being occupied by the tip of the inverted penis (Table 1, Figs 6–7), partially projected into the distal part of the female atrium in the holotype.

Epithelial lining of sperm ducts cuboidal and ciliated, becoming columnar in their distal expanded portions; thin muscularis (~3 µm thick) mainly constituted of circular fibres. Penis bulb constituted by a strong musculature containing interwoven circular and longitudinal fibres. Prostatic vesicle lined with columnar and ciliated epithelium. This epithelium receives abundant coarse granular, erythrophil secretion (Fig. 8*A*) as well as a few amount of fine granular, erythrophil secretion and of mixed secretion (an erythrophil central core and a cyanophil peripheral part). Both erythrophil secretions arise from cells bodies lying externally to the common muscle coat; the mixed secretion arises from glands with cells bodies internal to the common muscle coat. Muscularis of the prostatic vesicle is loosely arranged, constituted of interwoven longitudinal, circular and oblique fibres disposed among the numerous necks of the erythrophil cells. Ejaculatory cavity lined with columnar and ciliated epithelium (Fig. 8*A*). A sparse amount of fine xanthophil secretion is discharged into the proximal region of the ejaculatory cavity whereas abundant coarse granular, cyanophil secretion is discharged into its distal region. Both secretions arise from glands with bodies situated internal to the common muscle coat. Muscularis of ejaculatory cavity with interwoven circular and longitudinal fibres (~3 µm thick).

Epithelial lining of the lumen of inverted penis columnar, non-ciliated, with some insunk nuclei. Proximal half of inverted penis receives numerous coarse granular, xanthophil secretion (Fig. 8*B*) and sparse amount of cyanophil, amorphous secretion. Distal half of inverted penis receives two types of secretions: an amorphous, cyanophil secretion and a fine granular, erythrophil secretion (Fig. 8*C*, *D*). A short transition region (Fig. 8*B*) between proximal and distal halves receives abundant coarse granular, cyanophil secretion and a sparse amount of erythrophil secretion. All secretion types discharging into the lumen of inverted penis arise from glands located internal to the common muscle coat, usually among fibres of the muscularis. There is a loose connective tissue (~30 µm thick) (sponge-like tissue) under the epithelial lining of the distal half of the inverted penis (Fig. 8*C*). This tissue is better visualised in paratypes MZU PL.00139 and MZU PL.00141 (Fig. 6*A*, *B*) and contains nuclei of the insunk epithelial cells and scattered thin, circular muscle fibres as well

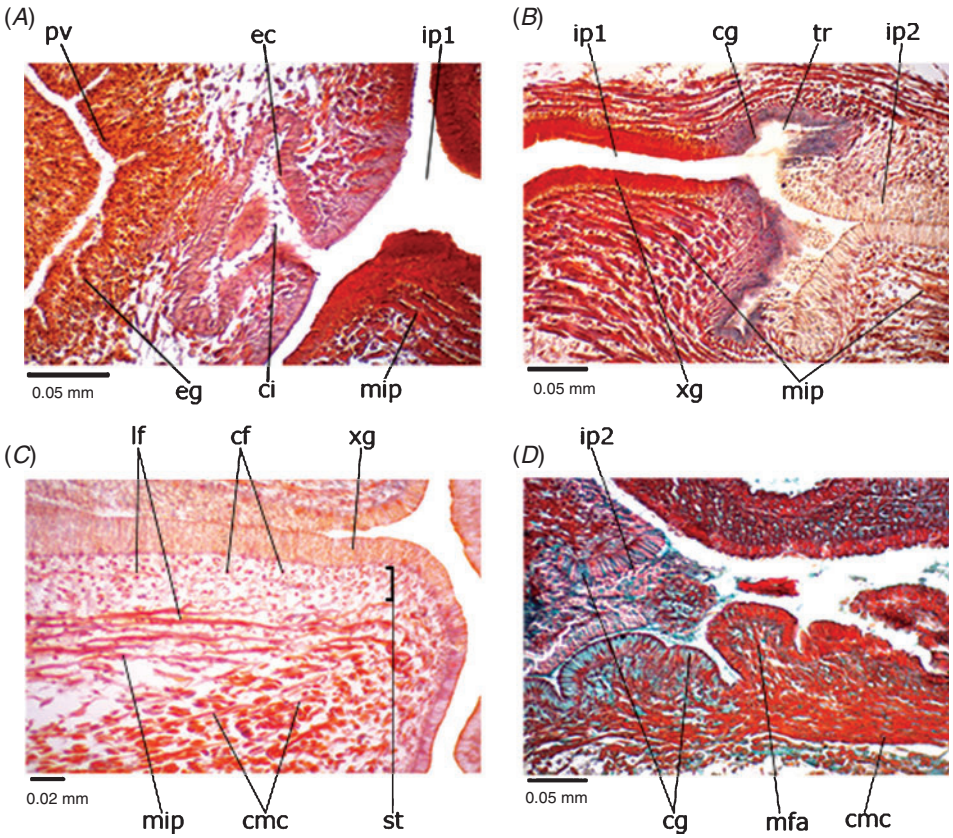

Fig. 8. *Choeradoplana minima*, sp. nov. Lemos & Leal-Zanchet: copulatory apparatus of the (*A*, *B*) paratype MZU PL.00141 and (*C, D*) holotype in sagittal sections. (*A*) Detail of the prostatic vesicle and ejaculatory cavity; (*B*, *C*) detail of the inverted penis; (*D*) female atrium. Anterior tip to the left. cf, circular muscle fibres; cg, cyanophil glands; ci, cilia; cmc, common muscle coat; ec, ejaculatory cavity; eg, erythrophil glands; ip1, proximal half of the inverted penis; ip2, distal half of the inverted penis; lf, longitudinal muscle fibres; mfa, muscularis of the female atrium; mip, muscularis of the inverted penis; pv, prostatic vesicle; st, sponge-like tissue; tr, transition region; xg, xanthophil glands.

as few longitudinal fibres. The muscularis, a strong mixed musculature, mainly containing longitudinal fibres, underlain this sponge-like tissue in the distal half of the atrium (60 µm thick) or the epithelium of the proximal half (50 µm−130 µm thick). Male atrium lined with columnar, non-ciliated epithelial cells. It receives three types of secretions: (1) fine granular, densely arranged in the cytoplasm, xanthophil secretion; (2) coarse granular, xanthophil secretion; (3) cyanophil amorphous secretion. Cyanophil glands have their cell bodies internal and/or externally to the common muscle coat; both types of xanthophil glands have their cell bodies situated internal to the common muscle coat. Muscularis of the male atrium with interwoven longitudinal and circular fibres (~5 µm); it is poorly defined from surrounding stroma.

Vitellaria, situated mainly between intestinal branches, open into the ovovitelline ducts. Ovaries oval-elongate in shape, measuring 0.24 mm anterior-posteriorly and 0.12 mm in diameter in the holotype. They are located immediately dorsal to the nerve plate. Ovovitelline ducts emerge from the lateral walls of the median third of ovaries (Fig. 5*F*), then recurve immediately dorsal to the nerve plate. Behind gonopore, the ovovitelline ducts ascend posteriorly and medially inclined, to unite dorsally to the proximal part of female atrium (proflex dorsal approach), thus forming the common glandular ovovitelline duct. Proximal portion of female atrium presents a short, dorso-anteriorly curved diverticulum (vagina) (Table 1). Female atrium oval-elongate, with folded wall (Figs 6–7,8*D*). Length of female atrium three times that of male atrium in the holotype (Table 1, Figs 6–7).

Paired ovovitelline ducts lined with cuboidal to columnar, ciliated epithelium and covered with a thin layer with interwoven circular and longitudinal muscle fibres (~4 µm thick). Common glandular ovovitelline duct lined with columnar ciliated epithelium; muscularcomprises intermingled circular and longitudinal muscle fibres (~15 µm thick). Abundant shell glands with xanthophil secretion open into distal ascending portion of paired ovovitelline ducts and common glandular ovovitelline duct (Figs 6–7).

Vagina and female atrium lined with columnar epithelium, higher in the vagina (~21 µm – 24 µm) than in the female atrium (~7 µm – 10 µm). Muscularis of female atrium and vagina comprised of circular subepithelial fibres and longitudinal subjacent fibres (6 µm). Muscularis of female atrium loosely arranged, poorly defined from surrounding stroma (Fig. 8*D*).

The most numerous glands discharging into the female atrium have a fine granular xanthophil secretion, densely arranged in the cytoplasm. In addition, there are a coarse granular, xanthophil secretion and a cyanophil amorphous secretion discharging into both the female atrium and the vagina, being more abundant in the distal region of the female atrium (Fig. 8*D*), near the gonopore. Both types of xanthophil secretion arise from cell bodies situated internal to the common muscle coat. Cyanophil glands have their cell bodies internal and/or externally to the common muscle coat.

Male and female atria with wide communication at the sagittal plane (Figs 6, 7). Gonopore canal nearly vertical at the sagittal plane (Figs 6, 7); it is lined with ciliated columnar epithelium and coated with circular fibres with subjacent longitudinal fibres (~9 µm). This canal receives two types of xanthophil secretion (fine granular, densely arranged in the cytoplasm, and coarse granular) as well as cyanophil amorphous secretion.

Common muscle coat strong, with interwoven oblique, circular and longitudinal fibres surrounding male and female atria, separated from the atrial muscularis by a stroma with variously oriented muscle fibres (Figs 8*C*, *D*). This stroma is stronger around female atrium than around male atrium. The muscular coats of male and female atria are independent, being more developed around the inverted penis (~60 µm–115 µm, ventrally and dorsally, respectively) than around female atrium (~50 µm).

Variation

Paratype MZU PL.00141 shows the inverted penis with a folded proximal half, whereas the distal half has longitudinal folds that restrict the lumen (Figs 6, 7, 8*B-C*). Similarly to the holotype, in paratypes MZU PL.00138, MZU PL.00139 and MZU PL.00142, the distal half of the inverted penis is partially projected into the distal part of the female atrium and/or the gonopore canal. In paratype MZU PL.00138, the epithelial lining of the distal region of the inverted penis covers the tip of the temporary papilla; the transition and the proximal regions are elongated, with tubular lumen and without folds, the transition region forming the lumen of the temporary papilla. A dorsal fold separating the atria occurs in paratypes MZU PL.00141 and MZU PL.00139, anterior (MZU PL.00141) or posterior (MZU PL.00139) to the gonopore level. Vitellaria are well developed in the holotype and in paratypes MZU PL.00139 and MZU PL.00141. They are poorly developed in paratype MZU PL.00143.

Remarks

Considering its colour pattern, *C. minima*, sp. nov. has a striped pattern similar to *C. bilix* Marcus, 1951, *C. marthae* Froehlich, 1955, *C. ehrenreich* Graff, 1899 and *C. gladismariae* Carbayo & Froehlich, 2012. Among these species, two broad lateral bands occur in *C. bilix*, *C. marthae* and *C. gladismariae* (Marcus 1951; Froehlich 1955*b*; Carbayo and Froehlich 2012). The latter also has a dark median stripe, which is absent in *C. minima*, *C. bilix* and *C. marthae*. Mature specimens of *C. minima* differ from the other *Choeradoplana* species by its shorter length.

In relation to the internal morphology, *C. minima*, sp. nov. is similar to other species of the genus by having a compact copulatory apparatus with an intrabulbar prostatic vesicle. *Choeradoplana bilix* and *C. bocaina* Carbayo & Froehlich, 2012 are exceptions due to an extrabulbar prostatic vesicle (Marcus 1951; Carbayo and Froehlich 2012). However, a unique character of *C. minima* among described Neotropical geoplanids is the occurrence of a penis with strong bulbar musculature and a long and folded intrapenial cavity. This cavity is underneath a vacuolated tissue with thin, circular muscle fibres and a strong mixed musculature with mainly longitudinal fibres. These characteristics indicate that this type of penis evolved in parallel with the inverted penis of other triclads. This type of male copulatory organ differs from the eversible type of penis of the type species of the genus, *C. iheringi*, in which the male atrium has an ample cavity and a folded wall without a vacuolated tissue and with a muscularis divided into a subepithelial circular layer and a subjacent longitudinal layer.

Distribution:

Rio Grande do Sul (São Francisco de Paula), Brazil.

Etymology

The specific epithet refers to the small length of mature specimens.

Choeradoplana benyai, sp. nov. Lemos & Leal-Zanchet

Choeradoplana sp. 3: Leal-Zanchet & Carbayo, 2000: 23.
Choeradoplana sp. 2: Leal-Zanchet & Baptista, 2009: 202.
Choeradoplana sp. 3 Leal-Zanchet, Baptista, Campos, & Raffo, 2011: 32.

Material examined

Holotype. MZUSP PL.1235: L. Guterres, *leg*. 05. X. 2003: São Francisco de Paula, RS, Brazil – anterior tip: transverse sections on 7 slides; anterior region at the level of ovaries: transverse sections on 54 slides; pre-pharyngeal region: transverse sections on 13 slides; pharynx: sagittal sections on 36 slides; copulatory apparatus: sagittal sections 36 slides;

Paratypes. MZU PL.00146: L. S. Teixeira, *leg*. 03. IV. 1998: São Francisco de Paula, RS, Brazil – anterior tip in three fragments: transverse and sagittal sections on 53 slides; pre-pharyngeal region: transverse sections on 9 slides; pharynx: sagittal sections on 14 slides; copulatory apparatus in three fragments: sagittal sections on 33 slides; MZU PL.00147: T. Fleck, *leg*. 25. XI. 1998: São Francisco de Paula, RS, Brazil – pre-pharyngeal region: transverse sections on 10 slides; pharynx: sagittal sections on 17 slides; copulatory apparatus: sagittal sections on 22 slides; MZU PL.00150: A. M. Leal-Zanchet, *leg*. 31. X. 2000: São Francisco de Paula, RS, Brazil – anterior tip: sagittal 6 slides; anterior region at the level of ovaries: horizontal sections on 10 slides; pre-pharyngeal region: transverse sections on 5 slides; pharynx: sagittal on 9 slides; copulatory apparatus: horizontal sections on 19 slides; MZU PL.00151: S. V. Amaral, *leg*. 21. III. 2010: São Francisco de Paula, RS, Brazil – anterior tip: transverse and sagittal sections on 243 slides; anterior region at the level of ovaries: horizontal sections on 7 slides; pre-pharyngeal region: transverse sections on 90 slides; pharynx: sagittal sections on 131 slides; copulatory apparatus: sagittal sections on 148 slides; posterior fragment preserved in ethanol 100% for molecular analyses; MZU PL.00152: I. H. Rossi, *leg*. 15. IX. 2012: São Francisco de Paula, RS, Brazil – copulatory apparatus: sagittal sections on 24 slides; posterior fragment preserved in ethanol 100% for molecular analyses.

Type locality:

São Francisco de Paula, state of Rio Grande do Sul (RS), Brazil.

Diagnosis

Dorsal surface dark-brown; eyes marginal, mainly pluriserial, without clear halos; mc:h, 17%–24%; sperm ducts opening into the lateral walls of prostatic vesicle; prostatic vesicle intrabulbar, globose, with high folds and narrow lumen in its anterior half; ejaculatory duct long; penis papilla long, cylindrical, with folded wall; male atrium short occupied by the proximal portion of the penis papilla; ovovitelline ducts emerging laterally from median third of ovaries, and ascending behind the gonopore; male and female atria with independent musculatures and with wide communication.

Description

External morphology

Body elongate with parallel margins (Figs 9–10*A*), subcylindrical in cross-section; anterior end obtuse, posterior end pointed. Cephalic region (4.5 mm long and 1.7 mm wide in the holotype with two glandular cushion and a median slit in the ventral surface. When crawling, maximal length reaches 60 mm (Table 3). Mouth distance from anterior tip, 66%, gonopore distance from anterior tip, 80% relatively to body length in the holotype (Table 3). Alive, dorsal surface dark-brown. Background colour light-brown, visible on a thin median stripe and margins of the body (Fig. 9), as well as on irregularly distributed spots. After fixation, the median stripe occurs in the anterior body third, being absent in the first 3 mm of the body (7% of body length). Ventral surface light-brown; glandular cushions dark-brown. In preserved specimens ground colour fades.

Sensorial border visible between the fourth and seventh millimetre of the body. Eyes absent on the first 3 mm of the body. Therefore they begin marginal and uniserial disposed, becoming pluriserial after the fourth millimetre of the body (Fig. 10*B*). They form three to four series. Towards posterior end, they become sparser, occurring until next to the posterior tip (Fig. 10*C*). No clear halos.

Fig. 9. *Choeradoplana benyai*, sp. nov. Lemos & Leal-Zanchet: photograph of live specimens in dorsal view: (*A*) paratype MZU PL. 00152; (*B*) holotype; and (*C*) paratype MZU PL. 00152. Arrows indicate the anterior tip.

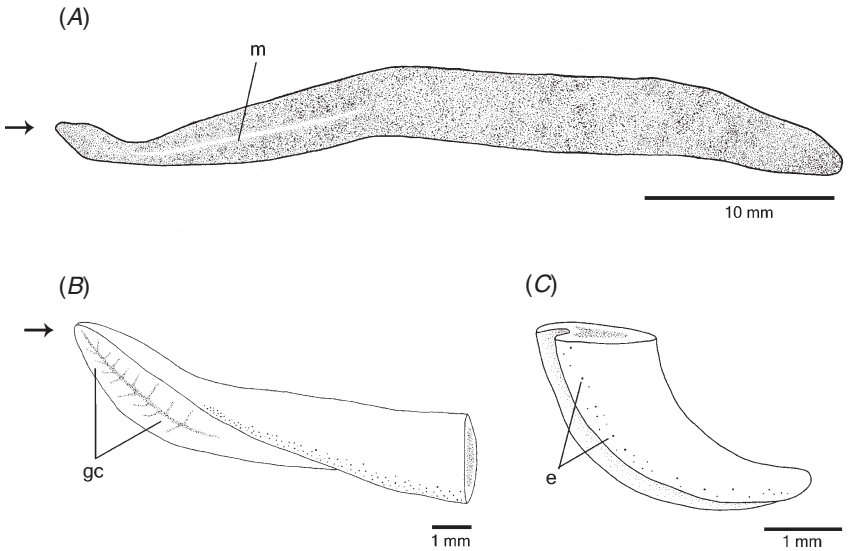

Fig. 10. *Choeradoplana benyai*, sp. nov. Lemos & Leal-Zanchet (holotype): (*A*) colour pattern in dorsal view; (*B*) detail of eyes pattern of the anterior body third in lateral view; (*C*) detail of the posterior body third in lateral view. Arrows indicate the anterior tip. e, Eyes; gc, glandular cushions; m, median stripe.

Table 3. Measurements, in millimetre, of specimens of *Choeradoplana benyai*, sp. nov. Lemos & Leal-Zanchet

–: not measured; *: After fixation; **: specimens with damaged anterior tip (lost or regenerating); DG: distance of gonopore from anterior end; DM: distance of mouth from anterior end; DMG: distance between mouth and gonopore; DPVP: distance between prostatic vesicle and pharyngeal pouch. The numbers given in parentheses represent the position relative to body length

	Holotype MZUSP PL. 1235	Paratype MZU PL. 00146	Paratype MZU PL. 00147	Paratype MZU PL. 00150	Paratype MZU PL. 00151	Paratype MZU PL. 00152
Maximum length in extension	60	55	47	50	60	45
Maximum width in extension	4	2.5	2	3	2	3
Length at rest	43	45	20	38	–	25
Width at rest	6	5	3	4	–	4
Length*	41	50	–	41	33	–
Width*	4	3.3	2.9	3	3	–
DM*	27 (66)	30.5 (61)	–	28.7 (70)	23.5 (71.2)	–
DG*	33 (80)	36.5 (73)	–	33.4 (81.5)	25 (75.7)	–
DMG*	6	6	4	3.8	1.5	–
DPVP*	–	1.8	1.2	1.2	0.6	–
Creeping sole %	90	82	59	77	73	–
Ovaries	11.6 (28.3)	8.7 (17.4)	–	10.1 (25)	–	–
Anteriormost testes	10.7 (26)	8.4 (16.8)	–	9.7 (24)	–	–
Posteriormost testes	25 (61)	28.7 (57)	–	27.6 (67)	23.5 (71)	–
Prostatic vesicle	0.8	1.3	1.3	1.2	–	–
Penis papilla	5.3	4.7	3.7	3.4	–	–
Male atrium	2.0	1.0	0.5	0.6	4.2	–
Female atrium	1.3	4.0	3.7	0.8	3.0	–
Vagina	0.6	0.6	0.4	0.2	0.1	–
Common ovovitelline duct	0.3	0.2	0.4	0.1	0.2	–

Internal morphology

Sensory organs, cutaneous and mesenchymal musculatures and epidermis

Sensory pits, as simple invaginations, ~16 µm to 30 µm deep, absent on anterior tip. They occur in a single row between 0.9 mm and 12 mm from anterior tip, at intervals from 50 µm to 230 µm. Eyes between 35 µm and 65 µm in diameter.

Cutaneous musculature with the usual three layers (circular, oblique and longitudinal layers), but with the ventral longitudinal layer partially insunk in the mesenchyme (Table 4, Fig. 11*A*, *B*). The longitudinal layer is approximately

Table 4. Cutaneous musculature and body height, in micrometre, in the median region of a transverse section of the pre-pharyngeal region, and ratio of the height of cutaneous musculature to the height of the body (mc:h index) of specimens of *Choeradoplana benyai*, sp. nov. Lemos & Leal-Zanchet

	Holotype MZUSP PL. 1235	Paratype MZU PL. 00146	Paratype MZU PL. 00147	Paratype MZU PL. 00150	Paratype MZU PL. 00151
Dorsal circular	6	3.7	3.7	2.5	5
Dorsal oblique	35	17.5	25	25.5	26.2
Dorsal longitudinal	215	200	125	100	162.5
Total Dorsal	256	221.2	153.7	128	193.7
Ventral circular	6	3.75	6.25	3.7	2.5
Ventral oblique	25	16.25	12.5	12.5	11.2
Ventral longitudinal	55	36.25	30	38.7	26.2
Ventral longitudinal insunk	60	58.75	43.75	41.2	43.7
Total Ventral	146	115	92.5	96.1	83.6
Body height	1675	1400	1150	960	1580
Mc:h (%)	24	24	21	23	17

about five times higher than the other two in the pre-pharyngeal region in the holotype (Table 4). Musculature higher medially, becoming progressively lower towards body margins (Fig. 11*A*, *B*). At the sagittal plane, dorsal musculature higher than the ventral in the pre-pharyngeal region (Fig. 11*A*). Mc:h 24% in the holotype (Table 4). The dorsal cutaneous musculature is thinner next to the anterior tip, whereas the ventral cutaneous musculature is higher and with the longitudinal layer totally insunk in the mesenchyme, located below cell bodies of glands opening through ventral epidermis, forming the retractor muscle (Fig. 11*C*).

Mesenchymal musculature well developed with variously oriented fibres, mainly forming three layers: oblique dorsal (~4–6 fibres thick), supra-intestinal transverse (~6–12 fibres thick) and sub-intestinal transverse (~6–12 fibres thick) (Fig. 11*A*). In addition, dorsoventral fibres are present. Longitudinal fibres are indiscernible. Fibres of the oblique dorsal and supra-intestinal layers form a dorsal muscle net ('Muskelgeflecht') in the cephalic region. The sub-intestinal transverse layer is thicker in the cephalic region than in the pre-pharyngeal region and interwoven with the fibres of the insunk ventral cutaneous musculature in the retractor muscle (Fig. 11*C*).

Width of creeping sole, 90% of body width in the holotype (Table 3). A slit occurs between the two glandular cushions in the cephalic region, representing the beginning of the creeping sole from 0.4 mm to 3 mm from anterior tip. Three types of secretory cells open through dorsal epidermis and body margins: (1) abundant rhabditogen cells with xanthophil secretion (rhammites); (2) sparse cells with fine granular, erythrophil secretion; (3) cells with amorphous, cyanophil secretion. Creeping sole receives abundant amorphous cyanophil secretion and scarce cells with fine granular, erythrophil secretion and small, xanthophil rhabdites. There is no glandular margin (Fig. 11*A*). Three gland types also open through the epidermis of the whole surface of the anterior tip (rhabditogen cells with rhammites; cells with fine granular, erythrophil secretion; and cells with amorphous, cyanophil secretion). Rhabditogen cells are more numerous on ventral surface of the anterior tip. Cell bodies of the glands opening on ventral surface are located between the retractor muscle and ventral epidermis forming the musculo-glandular organ next to the anterior tip (Fig. 11*C*, *D*).

Pharynx

Pharynx bell-form with folded wall. Mouth in the posterior half of pharyngeal pouch, slightly posterior to the dorsal insertion. Oesophagus absent (Fig. 11*E*). Pharynx and pharyngeal lumen lined by cuboidal to columnar ciliated epithelium showing some insunk nuclei; the insunk nuclei of the epithelium of the pharyngeal lumen are located immediately subepithelially or among fibres of inner pharyngeal musculature. Four types of pharyngeal glands: fine granular, xanthophil secretion; amorphous, cyanophil secretion; two types of erythrophil secretion (one with fine granular, loosely arranged in the cytoplasm; the other with coarse, densely arranged granules). Cell bodies of pharyngeal glands located in the mesenchyme, mainly anterior and posteriorly to pharynx. Outer musculature of pharynx (~40 µm thick) constituted of thin longitudinal subepithelial layer, followed by a thicker circular one, mixed internally with few longitudinal fibres. Towards pharyngeal tip, circular layer becomes as thin as longitudinal one. Inner pharyngeal musculature (~45 µm thick) composed of thick circular subepithelial layer mixed with some longitudinal fibres. Inner musculature gradually becomes thinner outwards and inwards.

Reproductive apparatus

Testes in two to three irregular rows on each side of the body, beneath the dorsal transverse mesenchymal muscles, embedded between intestinal branches (Fig. 11*A*). They extend from anterior of the ovaries to just anterior of the pharynx (Table 3). Pre-pharyngeally, sperm ducts dorsal to ovovitelline ducts, medianlly displaced. They form spermiducal vesicles posterior to pharynx. Spermiducal vesicles enter common muscle coat and ascend slightly to open into the lateral walls of prostatic vesicle (Figs 12, 13*C*). Intrabulbar prostatic vesicle globose, with high folds and narrow lumen (Table 3, Figs 12–14*A*). The prostatic vesicle narrows and penetrates the penis papilla

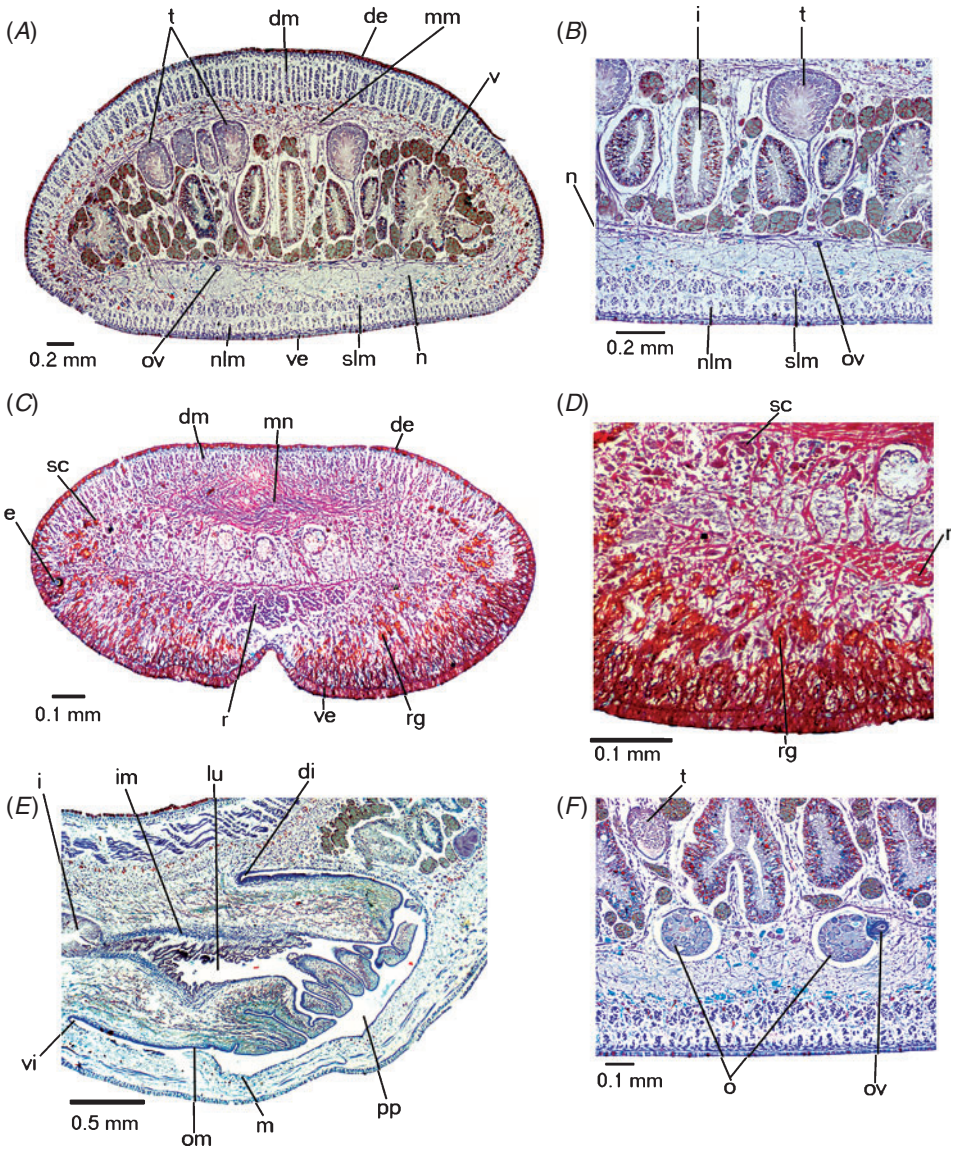

Fig. 11. *Choeradoplana benyai*, sp. nov. Lemos & Leal-Zanchet (holotype) in (*A–D*, *F*) transverse or (*E*) sagittal sections: (*A*) pre-pharyngeal region; (*B*) detail of the ventral surface of the pre-pharyngeal region; (*C*) anterior region of the body; (*D*) detail of ventral surface of the anterior region of the body; (*E*) pharynx; (*F*) ovaries. In *E*, anterior tip to the left. de, Dorsal epidermis; di, dorsal insertion; dm, dorsal cutaneous musculature; e, eyes; i, intestine; im, inner pharyngeal musculature; lu, pharyngeal lumen; m, mouth; mm, mesenchymal muscles; mn, muscle net; n, nerve plate; nlm, normal longitudinal cutaneous muscles; o, ovary; om, outher musculature of pharynx; ov, ovovitelline duct; pp, pharyngeal pouch; r, retractor muscle; rg, rhabditogen cells; sc, secretory cells; slm, sunken longitudinal cutaneous muscles; t, testes; v, vitellaria; ve, ventral epidermis; vi, ventral insertion.

forming a long ejaculatory duct which traverses the almost symmetrical penis papilla to open through its tip (Figs 12–14*C*). Penis papilla long, cylindrical, with folded wall. Male atrium short, with the entire cavity occupied by the proximal part of the penis papilla that extends into the female atrium (Table 3, Figs 12–14*C*).

Epithelial lining of sperm ducts cuboidal and ciliated; thin muscularis (~6 µm thick) mainly constituted of circular fibres. Penis bulb constituted by a strong musculature containing interwoven circular, diagonal and longitudinal fibres. Prostatic vesicle lined with columnar epithelium with few ciliated cells, excepting next to the transition to the ejaculatory duct, where the epithelium becomes densely ciliated. In the proximal half of the prostatic vesicle, the epithelium receives abundant coarse granular, xanthophil secretion (Fig. 14*A*), as well as sparse fine granular, erythrophil secretion. Both glands become sparse in the distal half of the prostatic vesicle. The xanthophil secretion arises from cells bodies lying externally to the common muscle coat; the erythrophil secretion arises from glands with cells bodies located between the fibres of the

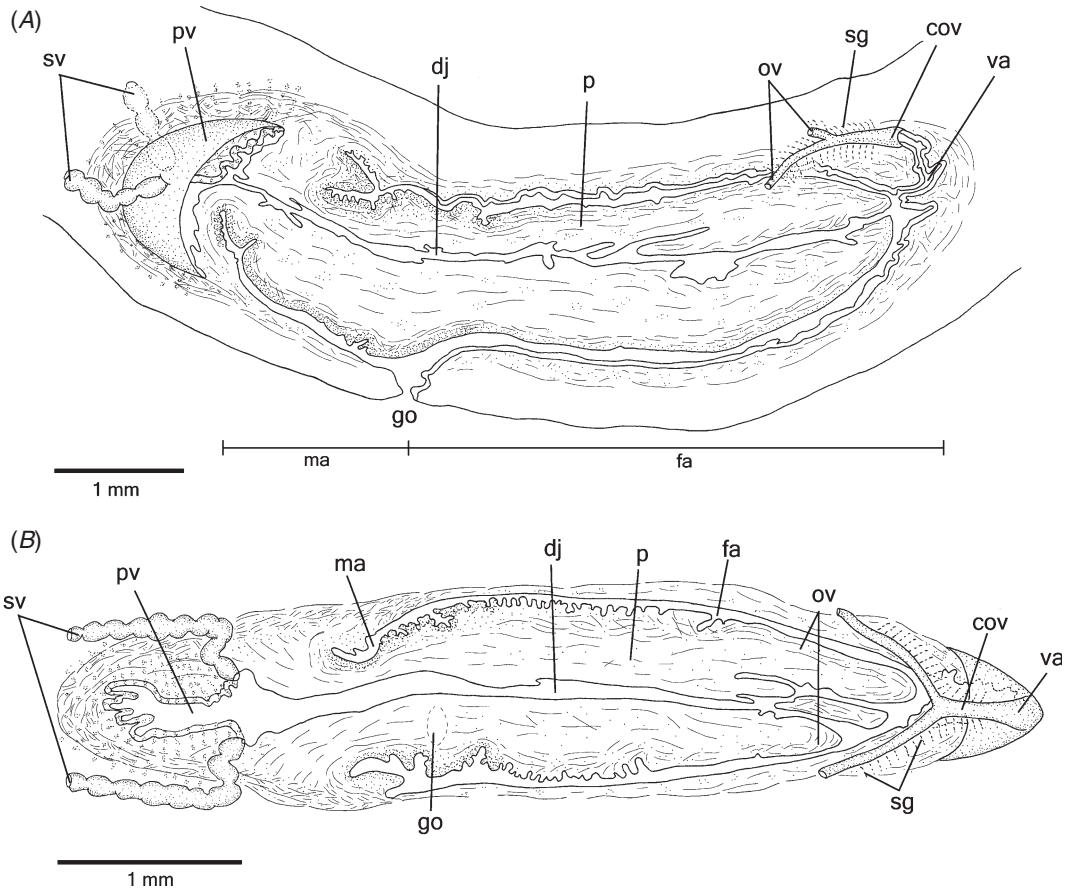

Fig. 12. *Choeradoplana benyai*, sp. nov. Lemos & Leal-Zanchet: (*A*) sagittal composite reconstruction of the copulatory apparatus of the holotype and (*B*) horizontal composite reconstruction of the copulatory apparatus of the paratype MZU PL. 00150. Anterior tip to the left. cov, Common glandular ovovitelline duct; ej, ejaculatory duct; fa, female atrium; go, gonopore; ma, male atrium; ov, ovovitelline ducts; p, penis papilla; pv, prostatic vesicle; sg, shell glands; sv, spermiducal vesicle; va, vagina.

common muscle coat or external to it. Muscularis of the prostatic vesicle is loosely arranged, constituted of interwoven longitudinal, circular and oblique fibres disposed among the numerous necks of the xanthophil cells. Ejaculatory duct lined with cuboidal and ciliated epithelium. A sparse amount of fine granular, erythrophil secretion, as well as cyanophil amorphous secretion, is discharged into ejaculatory duct. Both secretions arise from glands with intrapapillar bodies. Muscularis of ejaculatory duct with mainly longitudinal fibres (~5 µm–10 µm thick).

Penis papilla lined with columnar, non-ciliated epithelium. The proximal third of the penis papilla has low folds and receives numerous cyanophil amorphous secretion as well as sparse fine granular, weakly stained erythrophil secretion (Fig. 14*B*). Both glands have their cell bodies internal to the common muscle coat; the cell bodies of the cyanophil glands are characteristically subepithelial disposed. The other two-thirds of the penis papilla receive abundant fine granular, erythrophil secretion as well as cyanophil amorphous secretion. Both glands show intrapapillar cell bodies. Muscularis of the penis papilla, stronger distally (~25 µm – 50 µm in the proximal third and 80 µm – 200 µm in the other two-thirds), with subepithelial circular fibres and subjacent longitudinal fibres; longitudinal fibres more numerous in the median and distal thirds of the penis papilla.

Male atrium lined with cuboidal to columnar (Fig. 14*B*), non-ciliated epithelium, which becomes ciliated next to the gonopore canal. Two types of secretory cells, both sparse, open through the epithelium of the atrium: (1) cells with amorphous cyanophil secretion; (2) cells with fine granular, erythrophil secretion. Erythrophil secretion arises from glands located internal to the common muscle coat; cyanophil secretion arises from glands external to the muscle coat. Muscularis of the atrium mainly with subepithelial circular fibres and some subjacent longitudinal fibres (~10 µm).

Vitellaria, situated mainly between intestinal branches, open into the ovovitelline ducts. Ovaries ovoid in shape, measuring 0.3 mm anterior-posteriorly and 0.2 mm in diameter in the holotype. They are located immediately dorsal to the nerve plate. Ovovitelline ducts emerge from the lateral walls of the median third of ovaries (Fig. 11F), then recurve immediately dorsal to the nerve plate. Behind gonopore, the

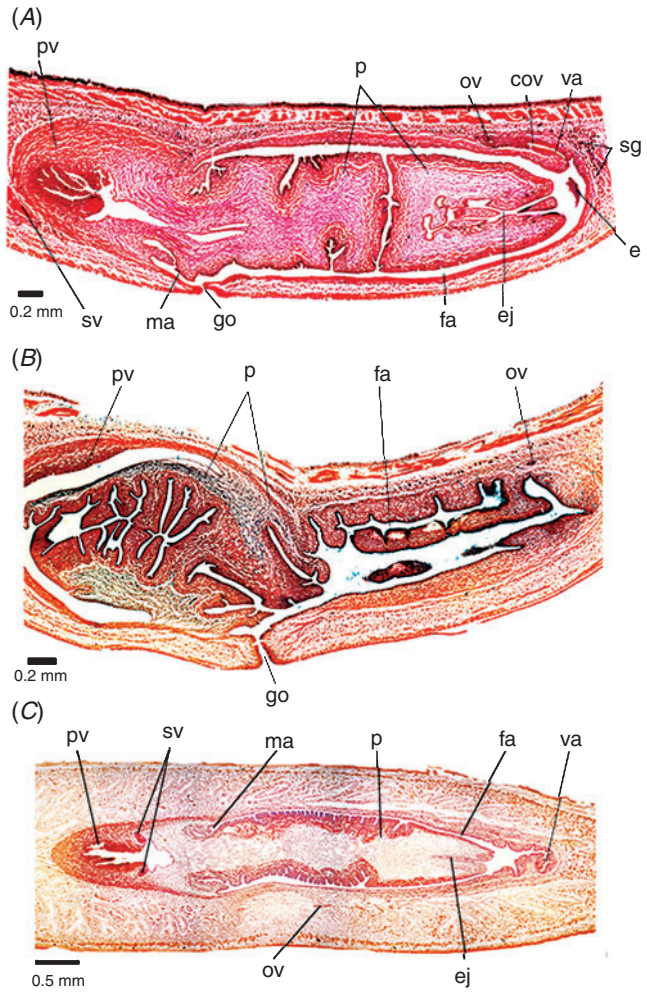

Fig. 13. *Choeradoplana benyai*, sp. nov. Lemos & Leal-Zanchet: copulatory apparatus in sagittal section of (*A*) paratypes MZU PL. 00147 and (*B*) MZU PL. 00151; (*C*) copulatory apparatus in horizontal section of the paratype MZU PL. 00150. Anterior tip to the left. cov, Common glandular ovovitelline duct; e, ejaculate; ej, ejaculatory duct; fa, female atrium; go, gonopore; ma, male atrium; ov, ovovitelline ducts; p, penis papilla; pv, prostatic vesicle; sg, shell glands; sv, spermiducal vesicle; va, vagina.

ovovitelline ducts ascend posteriorly and medially inclined, to unite dorsally to the proximal fourth of the atrium (proflex dorsal approach), thus forming the common glandular ovovitelline duct. Proximal portion of the atrium presents a long, dorso-anteriorly curved diverticulum (vagina) (Table 3, Figs 12, 13*A*, *C*, 14*C*). Atrium with almost unfolded wall, except for some low folds. Length of female atrium four times that of male atrium in the holotype (Table 1, Figs 12*A*, 14*A–C*).

Paired ovovitelline ducts lined with cuboidal to columnar, ciliated epithelium and covered with a thin layer with interwoven circular and longitudinal muscle fibres (~5 µm thick). Common glandular ovovitelline duct lined with columnar ciliated epithelium; musculacomprises intermingled circular and longitudinal muscle fibres (~10 µm thick). Abundant shell glands with xanthophil secretion open into distal ascending portion of paired ovovitelline ducts and common glandular ovovitelline duct (Figs 12–14*C*).

Female atrium and vagina lined mainly with columnar and non-ciliated epithelium that becomes higher and pseudostratified in the posterior half of the atrium as well as in the vagina. Epithelial lining of the female atrium may have insunk nuclei (Fig. 14*D*) and becomes ciliated next to the gonopore. Three types of secretory cells open through the epithelium of the atrium and vagina: (1) abundant cells with amorphous cyanophil secretion (Fig. 14*D*); (2) cells with coarse granular, xanthophil secretion; (3) cells with fine granular, erythrophil secretion. Xanthophil secretion arises from glands located internal to the common muscle coat; erythrophil and cyanophil secretions arise from glands with cell bodies near the muscle coat or external to it. Muscularis of the atrium and vagina mainly with interwoven circular and longitudinal fibres (~10 µm in the atrium and 5 µm – 25 µm in the vagina).

Gonopore canal vertical at the sagittal plane (Figs 12*A*, *B*, 13*A*); it is lined with ciliated columnar epithelium and coated with circular fibres and subjacent longitudinal fibres (~15 µm). This canal receives three types of secretion: fine granular, xanthophil; fine granular, erythrophil; cyanophil amorphous secretion.

Common muscle coat strong, especially where it forms the penis bulb (Figs 13*A*, 14*A*), with interwoven oblique, circular and longitudinal fibres. Around the atria, this coat is separated from the atrial muscularis by a stroma with variously oriented muscle fibres.

Variation

Paratype MZU PL.00151 has a contracted penis papilla that is retracted into a proximal bulbar cavity (Fig. 13*B*). The dilated prostatic vesicle forms the anterior wall and the expanded ejaculatory duct forms the posterior wall of this cavity. The epithelium of the external surface of the penis papilla lines a sinuous and folded cavity inside the contracted papilla. The female atrium has elongate longitudinal folds. Paratype MZU PL.00147 has the external surface of the penis papilla with folded indentations (Fig. 13*A*). The female atrium shows a kind of ejaculate (Fig. 13*A*) which contains erythrophil and cyanophil amorphous secretions mixed with holocrine secretion and clusters of erythrophil apocrine secretion of the prostatic vesicle. Sperm was not observed in the ejaculate. The epithelial lining of the female atrium shows cyanophil and erythrophil apocrine secretions. Vitellaria are well developed in the holotype MZU PL.00146 and in paratypes MZU PL.00147, MZU PL.00150 and MZU PL.00152. Both vitellaria and shell glands are poorly developed in paratype MZU PL.00151.

Remarks

The external features of *Choeradoplana benyai*, sp. nov. resemble those of dark specimens of the sympatric *C. iheringi*. Several times specimens of both species could not be distinguished one from another during fieldwork. However *C. benyai*, sp. nov. specimens are generally more intensively pigmented.

The copulatory apparatus of *C. benyai*, sp. nov. is unique in the genus in having the gonopore canal shifted anteriorly, near

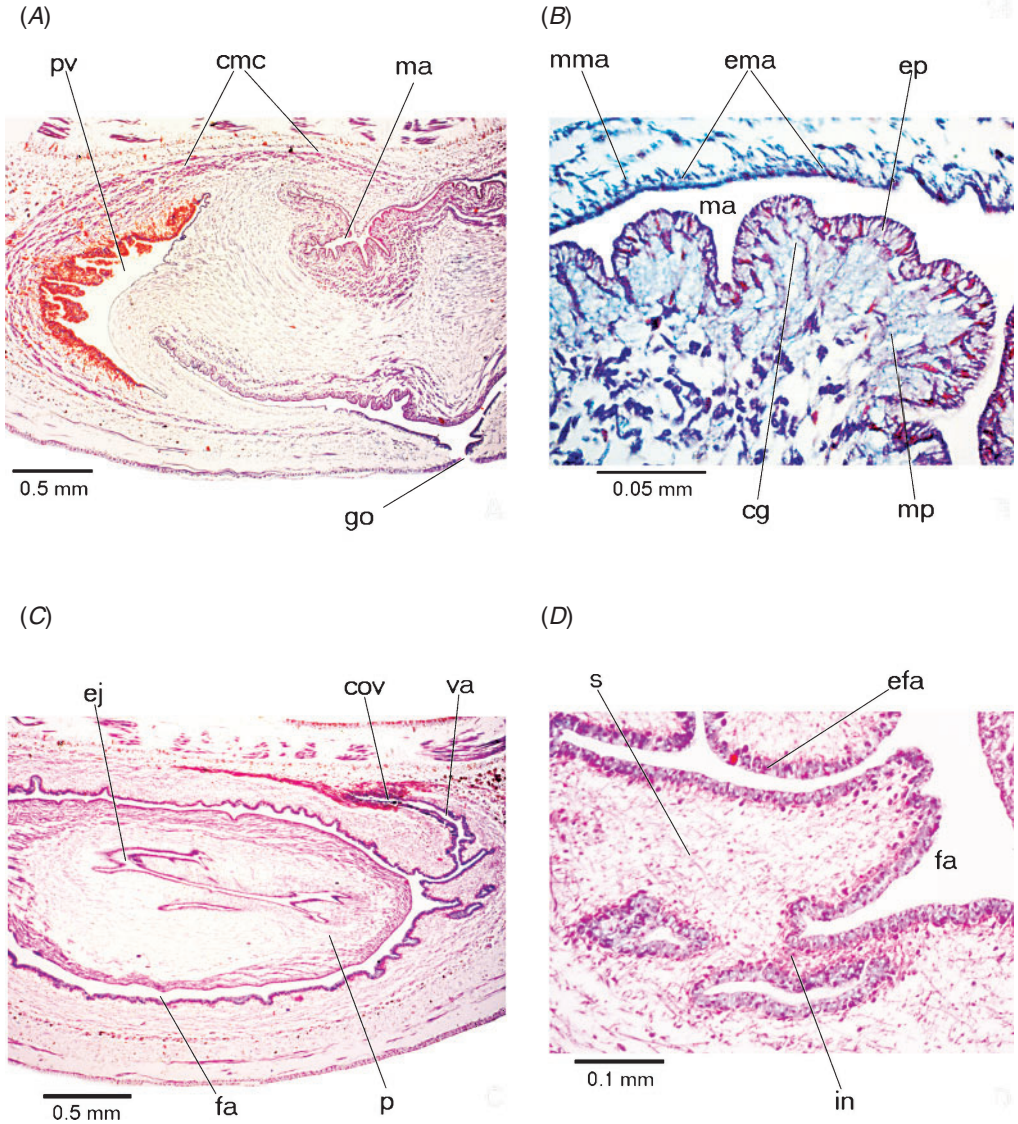

Fig. 14. *Choeradoplana benyai*, sp. nov. Lemos & Leal-Zanchet (holotype): copulatory apparatus in sagittal sections. (*A*) Prostatic vesicle and proximal part of the penis papilla in the male atrium; (*B*) detail of the male atrium and proximal part of the penis papilla, (*C*) female organs and distal part of the penis papilla in the female atrium; (*D*) detail of the female atrium. Anterior tip to the left. cg, cyanophil glands; cmc, common muscle coat; cov, common glandular ovovitelline duct; ep, lining epithelium of the penis papilla; efa, lining epithelium of the male atrium; ej, ejaculatory duct; ema, lining epithelium of the male atrium; fa, female atrium; go, gonopore; in, insunk nuclei; ma, male atrium; mma, muscularis of the male atrium; mp, muscularis of the penis papilla; p, penis papilla; pv, prostatic vesicle; s, stroma; va, vagina.

the level of the insertions of the penis papilla that is long and cylindrical and occupies the whole female atrium.

Distribution

Rio Grande do Sul (São Francisco de Paula), Brazil.

Etymology

The specific epithet refers to MSc. Edward Benya as acknowledgement to his collaboration with laboratory work and friendship.

Notes on ecology and distribution

Choeradoplana minima, sp. nov. and *C. benyai*, sp. nov. have been solely recorded in the National Forest of São Francisco de Paula, where they occur inside and on the borders of sites with the native vegetation (Mixed Ombrophilous Forest). In this conservation unit of sustainable use, constituted by a mosaic of native and exotic vegetation, many specimens were collected in sites of plantations of the native *Araucaria angustifolia*. Similarly to other species of land planarians, areas with plantations of exotic species (e.g. *Pinus* spp.) of the mosaic may be used as corridors (Fonseca *et al.* 2009). Thus, one

specimen of *C. minima* was collected in an area of *Pinus* plantation.

Both species of flatworms herein described seem to be endemic to their type locality since they were registered neither in other areas of Mixed Ombrophilous Forest of the Araucaria Plateau (Leal-Zanchet *et al*. 2011) nor in other forest types in southern Brazil (Castro and Leal-Zanchet 2005; Antunes *et al*. 2008; Baptista and Leal-Zanchet 2010).

Discussion and conclusions

Among Geoplaninae, the genus *Choeradoplana* is relatively well defined by morphological characters, such as a cephalic region that is curved backwards, the occurrence of a cephalic glandulo-muscular organ and a cutaneous longitudinal musculature with a portion internal to the subcutaneous nerve plexus throughout the body, among others (Ogren and Kawakatsu 1990; Carbayo and Froehlich 2012; Carbayo *et al*. 2013). Thus, the morphological analyses alone strongly support the inclusion of the two new species into *Choeradoplana*. Similarly, ITS-1 differences among the species *C. minima*, sp. nov. and *C. benyai*, sp. nov. and the type species, *C. iheringi*, and measures of intraspecific and interspecific variation of the COI gene and ABGD supported the separation of these flatworms as evolutionarily independent species belonging to the genus *Choeradoplana.* Regarding relationships within taxa, results indicated that the COI gene should not be used for phylogenetic reconstruction above the species level, since all analyses did not indicate the inclusion of *C. bocaina* in the genus *Choeradoplana* in contrast to the results of Carbayo *et al*. (2013). Bayesian and ML analyses of the concatenation of ITS-1 and COI provided highly congruent and well resolved topologies, which confirm the close relationship between the genera *Choeradoplana* and *Cephaloflexa* as shown by Carbayo *et al*. (2013).

The copulatory apparatus of species of *Choeradoplana* is highly diverse (Froehlich 1955*b*; Carbayo and Froehlich 2012) and both species herein described, by presenting two different types of male copulatory organs, augment the known disparity. Many species of *Choeradoplana*, such as *C. iheringi*, *C. banga* Carbayo and Froehlich 2012, *C. gladismariae*, *C. bocaina* and possibly *C. langi*, have an eversible penis, with the male atrium forming numerous folds that project into the ample cavity. *Choeradoplana bilix*, *C. marthae* and *C. crassiphala* Negrete & Brusa, 2012 have a small conical penis papilla that occupies almost the whole male atrium cavity that is short and unfolded. *Choeradoplana minima*, sp. nov. has an inverted-type of penis that seems to be until now unknown in Geoplaninae. This type of penis is mainly characterised by histological details, such as a tubular cavity underneath by a vacuolated tissue with thin, circular muscle fibres underlain by a strong mixed musculature mainly with longitudinal fibres. In addition, the muscular coat is independent between male and female atria and is highly developed around the male atrium. *Choeradoplana catua* Froehlich, 1955, which also has a tubular cavity projecting anteriorly and as a type of bulbar cavity (of which the histological details are unknown), may have a penis that is similar to that of *C. minima*. An inverted type of penis also occurs in other triclads, such as the maricolan *Centriovarioplana tenuis* Westblad, 1952 (Sluys 1989) and the continenticolan *Eudoxiatopoplona bilaticlavia* Winsor, 2009 and *Marionfyfea*, among others (Winsor 2006, 2009). *Choeradoplana benyai*, sp. nov. possesses a gonopore shifted anteriorly and a long and cylindrical penis papilla, which are features that occur in species of other Geoplaninae genera, such as *Geoplana* and *Obama* (Froehlich 1959; Amaral *et al*. 2012; Carbayo *et al*. 2013), but until now were unknown in *Choeradoplana*.

Choeradoplana benyai and the type species of the genus, *C. iheringi*, are cryptic species occurring sympatrically in the São Francisco de Paula National Forest. These species can hardly be differentiated without analysing the morphology of their copulatory apparatuses, which is similar to the case of *C. banga* and *C. iheringi* (Carbayo and Froehlich 2012). *Choeradoplana iheringi* was described by Graff (1899) based on specimens from Taquara, southern Brazil, a locality near the São Francisco de Paula National Forest. This species seems to have an ample distribution in areas of Mixed Ombrophilous Forest in southern Brazil (Leal-Zanchet *et al*. 2011). The species was redescribed by Marcus (1951), based on specimens found in São Paulo state that had an external morphology similar to that of *C. iheringi*. Leal-Zanchet and Souza (2003) analysed specimens from São Paulo state and southern Brazil and also considered that the specimens of both areas are conspecific despite some anatomical and histological details that were assigned to populational differences. Molecular analyses of two specimens of *C. iheringi* from São Paulo state by Carbayo *et al*. (2013) indicated that the taxon is paraphyletic. In the present work, ABGD indicated the close relationship between the specimen KC608293.1, identified by Carbayo *et al*. 2013 as '*Choeradoplana iheringi sensu* Souza & Leal-Zanchet, 2003 540', and specimens of *C. banga*, but without differentiating them at the species level. Considering that *C. banga* and *C. iheringi* could be easily differentiated by their copulatory apparatuses, future analyses using morphological and molecular data, based on a larger dataset, should be used to solve this question, as suggested by Carbayo *et al*. (2013).

The results reinforce the need for studies on the internal morphology of land planarians for species identification, even in areas where the land flatworm fauna is well known. Morphological studies alone may be sufficient for species identification when mature specimens are available. However, since the main morphological features that differentiate *C. benyai*, sp. nov. from *C. iheringi* are found in the copulatory organs, immature specimens of these species can only be identified using molecular analyses.

Acknowledgements

We thank the Coordenação de Aperfeiçoamento de Pessoal de Nível Superior (CAPES) for a PhD scholarship to Virgínia Silva Lemos which contributed to the completion of this work. We acknowledge the Fundação de Amparo à Pesquisa do Rio Grande do Sul (FAPERGS) and the Conselho Nacional de Desenvolvimento Científico e Tecnológico (CNPq), for financial support and grants which contributed to an integrated research project in the São Francisco de Paula National Forest. We thank IBAMA and Instituto Chico Mendes for research permission and facilities granted for this National Forest. We also thank Letícia Guterres and Rafaela Canello, Universidade do Vale do Rio dos Sinos, for section preparation and all those who collaborated with specimen collection. Dr Lisandro Negrete,

Universidad de La Plata, Argentina, is acknowledged for the photo of the external morphology of *Choeradoplana benyai* in Fig. 9a. Ilana Rossi, Universidade do Vale do Rio dos Sinos, is thanked for the composite reconstruction of the external morphology of both species and her help with the final version of the figures. Emily Toriane is thanked for the English review. Dr Leigh Winsor, James Cook University, Australia, Dr Lizandra Jaqueline Robe, Universidade Federal de Rio Grande (FURG), Brazil, and two anonymous reviewers are gratefully acknowledged for their valuable comments and suggestions on an earlier version of this manuscript.

References

Akaike, H. (1974). A new look at the statistical model identification. *IEEE Transactions on Automatic Control* **19**, 716–723. doi:10.1109/TAC.1974.1100705

Álvarez-Presas, M., Carbayo, F., Rozas, J., and Riutort, M. (2011). Land planarians (Platyhelminthes) as a model organism for fine-scale phylogeographic studies: understanding patterns of biodiversity in the Brazilian Atlantic Forest hotspot. *Journal of Evolutionary Biology* **24**, 887–896. doi:10.1111/j.1420-9101.2010.02220.x

Amaral, V. S., Oliveira, S. M., and Leal-Zanchet, A. M. (2012). Three new species of land flatworms and comments on a complex of species in the genus *Geoplana* Stimpson (Platyhelminthes: Continenticola). *Zootaxa* **3338**, 1–32. http://www.mapress.com/zootaxa/2012/f/z03338p032f.pdf

Antunes, M. B., Marques, D. I. L., and Leal-Zanchet, A. M. (2008). Composição das comunidades de planárias terrestres (Platyhelminthes, Tricladida, Terricola) em duas áreas de floresta estacional decidual do sul do Brasil. *Neotropical Biology and Conservation* **31**, 34–38. doi:10.1590/S1676-06032010000200027

Antunes, M. B., Leal-Zanchet, A. M., and Fonseca, C. R. (2012). Habitat structure, soil properties, and food availability do not predict terrestrial flatworms occurrence in Araucaria Forest sites. *Pedobiologia* **55**, 25–31. doi:10.1016/j.pedobi.2011.09.010

Baguñà, J., Carranza, S., Pala, M., Ribera, C., Giribet, G., Arnedo, M., Ribas, M., and Riutort, M. (1999). From morphology and kariology to molecules. New methods for taxonomical identification of asexual populations of freshwater planarians. A tribute to Professor Mario Benazzi. *The Italian Journal of Zoology* **66**, 207–214. doi:10.1080/11250009909356258

Baptista, V. A., and Leal-Zanchet, A. M. (2005). Nova espécie de *Geoplana* Stimpson (Platyhelminthes, Tricladida, Terricola) do sul do Brasil. *Revista Brasileira de Zoologia* **22**, 875–882. doi:10.1590/S0101-81752005000400011

Baptista, V. A., and Leal-Zanchet, A. M. (2010). Land flatworm community structure in a subtropical deciduous forest in Southern Brazil. *Belgian Journal of Zoology* **140**, 83–90. [Accessed on August 2014]

Carbayo, F., and Froehlich, E. M. (2012). Three new Brazilian species of the land planarian *Choeradoplana* (Platyhelminthes: Tricladida: Geoplaninae), and an emendation of the genus. *Journal of Natural History* **46**, 1153–1177. doi:10.1080/00222933.2012.657699

Carbayo, F., and Leal-Zanchet, A. M. (2001). A new species of terrestrial planarian (Platyhelminthes, Tricladida, Terrestrial) from South Brazil. *Brazilian Journal of Biology* **61**, 437–447. doi:10.1590/S1519-69842001000300013

Carbayo, F., and Leal-Zanchet, A. M. (2003). Two new genera of geoplaninid land planarians (Platyhelminthes: Tricladida: Terricola) of Brazil in the light of cephalic specialisations. *Invertebrate Systematics* **17**, 449–468. doi:10.1071/IT01035

Carbayo, F., Leal-Zanchet, A. M., and Vieira, E. M. (2002). Flatworms (Platyhelminthes, Tricladida, Terricola) diversity versus man-induced disturbance in ombrophilous rainforest from Southern Brazil. *Biodiversity and Conservation* **11**, 1091–1104. doi:10.1023/A:1015865005604

Carbayo, F., Álvarez-Presas, M., Olivares, C. T., Marques, F. P. L., Froehlich, E. M., and Riutort, M. (2013). Molecular phylogeny of Geoplaninae (Platyhelminthes) challenges current classification: proposal of taxonomic actions. *Zoologica Scripta* **42**, 508–528. doi:10.1111/zsc.12019

Carranza, S., Littlewood, D. T. J., Clough, K. A., Ruiz, I., Baguñà, J., and Riutort, M. (1998). A robust molecular phylogeny of the Tricladida (Platyhelminthes, Seriata) and a reassessment of morphological synapomorphies. *Proceedings. Biological Sciences* **265**, 631–640. doi:10.1098/rspb.1998.0341

Castro, R. A., and Leal-Zanchet, A. M. (2005). Composição de comunidades de planárias terrestres (Platyhelminthes) em áreas de Floresta Estacional Decidual e de Campo na região central do Rio Grande do Sul, Brasil. *Acta Biologica Leopoldensia* **27**, 147–150. [Accessed on August 2014]

Du Bois-Reymond Marcus, E. (1951). On south american geoplanids. *Boletim da Faculdade de Filosofia Ciências e Letras da Universidade de São Paulo, série Zoologia* **16**, 217–255.

Felsenstein, J. (1985). Confidence limits on phylogenies: an approach using the bootstrap. *Evolution* **39**, 783–793. doi:10.2307/2408678

Fonseca, C. R., Ganade, G., Baldissera, R., Becker, C. G., Boelter, C. R., Brescovit, A. D., Campos, L. M., Fleck, T., Fonseca, V. S., Hartz, S. M., Joner, F., Kaffer, M. I., Leal-Zanchet, A. M., Marcelli, M. P., Mesquita, A. S., Mondin, C. A., Paz, C. P., Petry, M. V., Piovensan, S. M., Putzke, J., Stranz, A., Vergara, M., and Vieira, E. M. (2009). Towards an ecologically sustainable forestry in the Atlantic Forest. *Biological Conservation* **142**, 1209–1219. doi:10.1016/j.biocon.2009.02.017

Froehlich, C. G. (1955*a*). On the biology of land planarians. *Boletim da Faculdade de Filosofia Ciências e Letras da Universidade de São Paulo, série Zoologia* **20**, 263–272.

Froehlich, C. G. (1955*b*). Sobre a Morfologia e Taxonomia das Geoplanidae. *Boletim da Faculdade de Filosofia, Ciências e Letras. Série Zoologia* **19**, 195–279.

Froehlich, C. G. (1959). On Geoplanids from Brazil. *Boletim da Faculdade de Filosofia, Ciências e Letras. Série Zoologia.* **22**, 201–242.

Froehlich, E. M., and Leal-Zanchet, A. M. (2003). A new species of terrestrial planarian of the genus *Notogynaphallia* Ogren & Kawakatsu (Platyhelminthes, Tricladida, Terricola) from south Brazil and some comments on the genus. *Revista Brasileira de Zoologia* **20**, 745–753. doi:10.1590/S0101-81752003000400030

Graff, L. V. (1896). Über das System und die geographische Verbreitung der Landplanarien. *Verhandlungen der deutschen zoologischen Gesellschaft* **6**, 61–75.

Graff, L. V. (1899). 'Monographie der Turbellarien: II. Tricladida Terricola.' (Engelmann, Leipzig, Germany.)

Guindon, S., and Gascuel, O. (2003). A simple, fast, and accurate algorithm to estimate large phylogenies by maximum likelihood. *Systematic Biology* **52**, 696–704. doi:10.1080/10635150390235520

Hall, T. A. (1999). BioEdit: a user-friendly biological sequences alignment editor and analysis program for Windows 95/98/NT. *Nucleic Acids Symposium Series* **41**, 95–98.

Hasegawa, M., Kishino, H., and Yano, T. (1985). Dating of the human-ape splitting by a molecular clock of mitochondrial DNA. *Journal of Molecular Evolution* **22**, 160–174. doi:10.1007/BF02101694

Jones, H. D., and Cumming, M. S. (1998). Feeding behaviour of the termite-eating planarian *Microplana termitophaga* (Platyhelminthes: Turbellaria: Tricladida: Terricola) in Zimbabwe. *Journal of Zoology* **245**, 53–64. doi:10.1111/j.1469-7998.1998.tb00071.x

Katoh, K., and Toh, H. (2008). Recent developments in the MAFFT multiple sequence alignment program. *Briefings in Bioinformatics* **9**, 286–298. doi:10.1093/bib/bbn013

Kawaguti, S. (1932). On the physiology of land planarians. III. The problems of desiccation. *Memoirs of the Faculty of Science and Agriculture* **7**, 39–55.

Kimura, M. (1980). A simple method for estimating evolutionary rates of base substitution through comparative studies of nucleotide sequences. *Evolution* **16**, 111–120. doi:10.1007/BF01731581

Lázaro, E. M., Sluys, R., Pala, M., Stocchino, G. A., Baguñà, J., and Riutort, M. (2009). Molecular barcoding and phylogeography of sexual and asexual freshwater planarians of the genus Dugesia in the Western Mediterranean (Platyhelminthes, Tricladida, Dugesiidae). *Molecular Phylogenetics and Evolution* **52**, 835–845. doi:10.1016/j.ympev.2009.04.022

Leal-Zanchet, A. M., and Baptista, V. A. (2009). Planárias terrestres (Platyhelminthes: Tricladida) em áreas de floresta com araucária no Rio Grande do Sul. In 'Floresta com Araucária: Ecologia, Conservação e Desenvolvimento Sustentável.' (Eds C. R. S. Fonseca, A. F. Souza, T. L. Dutra, A. M. Leal-Zanchet, A. Backes and G. M. S. Ganade) pp. 199–207. (Holos, Ribeirão Preto, Brazil).

Leal-Zanchet, A. M., and Carbayo, F. (2000). Fauna de planárias terrestres (Platyhelminthes, Tricladida, Terricola) da Floresta Nacional de São Francisco de Paula, RS, Brasil: Uma análise preliminar. *Acta Biologica Leopoldensia* **22**, 19–25.

Leal-Zanchet, A. M., and Carbayo, F. (2001). Two new species of Geoplanidae (Platyhelminthes, Tricladida, Terricola) of South Brazil. *Journal of Zoology* **253**, 433–446. doi:10.1017/S0952836901000401

Leal-Zanchet, A. M., and Souza, S. A. (2003). Redescrição de *Choeradoplana iheringi* Graff (Platyhelminthes, Tricladida, Terricola). *Revista Brasileira de Zoologia* **20**, 523–530. doi:10.1590/S0101-81752003000300026

Leal-Zanchet, A. M., Baptista, V., Campos, L. M., and Raffo, J. F. (2011). Spatial and temporal patterns of land flatworms assemblages in Brazilian Araucaria forests. *Invertebrate Biology* **130**, 25–33. doi:10.1111/j.1744-7410.2010.00215.x

Leal-Zanchet, A. M., Rossi, I., Seitenfus, A. L. R., and Alvarenga, J. (2012). Two new species of land flatworms and comments on the genus *Pasipha* Ogren & Kawakatsu, 1990 (Platyhelminthes: Continenticola). *Zootaxa* **3583**, 1–21. [Accessed on August 2014]

Lemos, V. S., and Leal-Zanchet, A. M. (2008). Two new species of *Notogynaphallia* Ogren & Kawakatsu (Platyhelminthes: Tricladida: Terricola) from Southern Brazil. *Zootaxa* **1907**, 28–46. [Accessed on August 2014]

Marcus, E. (1951). Turbellaria brasileiros (9). *Boletim da Faculdade de Filosofia, Ciências e Letras da Universidade de São Paulo. Série Zoologia* **16**, 1–217.

Negrete, L., and Brusa, F. (2012). *Choeradoplana crassiphalla* sp. nov. (Platyhelminthes: Tricladida: Geoplanidae): a new species of land planarian from the Atlantic Forest of Argentina. *Studies on Neotropical Fauna and Environment* **47**, 227–237. doi:10.1080/01650521.2012.735071

Ogren, R. E. (1995). Predation behaviour of land planarians. *Hydrobiologia* **305**, 105–111. doi:10.1007/BF00036370

Ogren, R. E., and Kawakatsu, M. (1990). Index to the species of the family Geoplanidae (Turbellaria, Tricladida, Terricola) Part I: Geoplaninae. *Bulletin of the Fuji Women's College. Ser. II* **28**, 79–166.

Oliveira, S. M., Boll, P. K., Baptista, V. A., and Leal-Zanchet, A. M. (2014). Effects of pine invasion on land planarian communities in an area covered by *Araucaria* moist forest. *Zoological Studies* **53**, 19. doi:10.1186/s40555-014-0019-1

Posada, D., and Crandall, K. A. (1998). Modeltest: Testing the model of DNA substitution. *Bioinformatics* **14**, 817–818. doi:10.1093/bioinformatics/14.9.817

Prasniski, M. E. T., and Leal-Zanchet, A. M. (2009). Predatory behavior of the land flatworm Notogynaphallia abundans (Platyhelminthes: Tricladida). *Zoologia* **26**, 606–612. http://www.scielo.br/pdf/zool/v26n4/aop1109 [Accessed on August 2014]

Puillandre, N., Lambert, A., Brouillet, S., and Achaz, G. (2012). ABGD, Automatic Barcode Gap Discovery for primary species delimitation. *Molecular Ecology* **21**, 1864–1877. doi:10.1111/j.1365-294X.2011.05239.x

Rodríguez, F. J., Oliver, J. L., Marín, A., and Medina, J. R. (1990). The general stochastic model of nucleotide substitution. *Journal of Theoretical Biology* **142**, 485–501. doi:10.1016/S0022-5193(05)80104-3

Ronquist, F., and Huelsenbeck, J. P. (2003). MrBayes 3: Bayesian phylogenetic inference under mixed models. *Bioinformatics* **19**, 1572–1574. doi:10.1093/bioinformatics/btg180

Sluys, R. (1989). 'A Monograph of the Marine Triclads.' (A. A. Balkema: Rotterdam, The Netherlands.)

Sluys, R. (1995). Platyhelminthes as paleogeographical indicators. *Hydrobiologia* **305**, 49–53. doi:10.1007/BF00036362

Sluys, R., Kawakatsu, M., Riutort, M., and Baguñà, J. (2009). A new higher classification of planarian flatworms (Platyhelminthes, Tricladida). *Journal of Natural History* **43**, 1763–1777. doi:10.1080/00222930902741669

Talavera, G., and Castresana, J. (2007). Improvement of phylogenies after removing divergent and ambiguously aligned blocks from protein sequence alignments. *Systematic Biology* **56**, 564–577. doi:10.1080/10635150701472164

Winsor, L. (2006). New and revised terrestrial flatworm taxa (Platyhelminthes: Tricladida: Terricola) of Australia and the Subantarctic Islands of New Zealand. *Tuhinga: Records of the Museum of New Zealand Te Papa Tongarewa* **17**, 81–104.

Winsor, L. (2009). A new subfamily, new genus and new species of terrestrial flatworm (Platyhelminthes: Tricladida: Geoplanidae) from Stewart Island, New Zealand. *Tuhinga: Records of the Museum of New Zealand Te Papa Tongarewa* **20**, 23–32. http://www.tepapa.govt.nz/SiteCollectionDocuments/Tuhinga/Tuhinga20_023_Winsor.pdf

Winsor, L., Johns, P. M., and Yeates, G. W. (1998). Introduction, and ecological and systematic background, to the Terricola (Tricladida). *Pedobiologia* **42**, 389–404.

Xia, X., and Xie, Z. (2001). DAMBE: Software package for data analysis in molecular biology and evolution. *The Journal of Heredity* **92**, 371–373. doi:10.1093/jhered/92.4.371